Vol. 29 (1998) *ACTA PHYSICA POLONICA B* No 6

EXTENDED SMOLUCHOWSKI MODELS FOR INTERPRETING RELAXATION PHENOMENA IN LIQUIDS*

A. Polimeno, D. Frezzato, G. Saielli
G.J. Moro and P.L. Nordio

Department of Physical Chemistry, University of Padova
Via Loredan 2, 35131 Padova, Italy

(Received March 19, 1998)

Interpretation of the dynamical behaviour of single molecules or collective modes in liquids has been increasingly centered, in the last decade, on complex liquid systems, including ionic solutions, polymeric liquids, supercooled fluids and liquid crystals. This has been made necessary by the need of interpreting dynamical data obtained by advanced experiments, like optical Kerr effect, time dependent fluorescence shift experiments, two-dimensional Fourier-transform and high field electron spin resonance and scattering experiments like quasi-elastic neutron scattering. This communication is centered on the definition, treatment and application of several extended stochastic models, which have proved to be very effective tools for interpreting and rationalizing complex relaxation phenomena in liquids structures. First, applications of standard Fokker–Planck equations for the orientational relaxation of molecules in isotropic and ordered liquid phase are reviewed. In particular attention will be focused on the interpretation of neutron scattering in nematics. Next, an extended stochastic model is used to interpret time-domain resolved fluorescence emission experiments. A two-body stochastic model allows the theoretical interpretation of dynamical Stokes shift effects in fluorescence emission spectra, performed on probes in isotropic and ordered polar phases. Finally, for the case of isotropic fluids made of small rigid molecules, a very detailed model is considered, which includes as basic ingredients a Fokker–Planck description of the molecular librational motion and the slow diffusive motion of a persistent cage structure together with the decay processes related to the changing structure of the cage.

PACS numbers: 05.40. +j, 25.40. Fq, 33.50. Dq, 39.30. +w

* Presented at the Marian Smoluchowski Symposium on Statistical Physics, Zakopane, Poland, September 1–10, 1997.

1. Introduction

Simulations and theoretical studies of liquid structures are nowadays focused on complex liquids, including ionic fluids or melted salts, macromolecular fluids like polymers, and oriented phases. Investigations based on Molecular Dynamics or Montecarlo techniques are the main tool for testing microscopic theories of the liquid state, due to the rapid growth of computational power and the availability of realistic potential functions. However, the complexity of phenomena revealed by simulations and the difficulties which could arise in relating simulated results with actual experimental observations of dynamical observables in liquids, make way to the necessity of employing simplified models. Mesoscopic or stochastic models are suitable tools to interpret qualitatively, and often quantitatively, complex dynamical behaviours in liquids.

Extended stochastic models are particularly useful, since they include two main sets of degrees of freedom, namely rotational and/or translational variables of primary interest which describe the motion of single molecules sorted out as 'probes' or 'solute' and a set of additional variables of collective nature, related to solvation spheres, solvent polarization components and cage structures [1–4]. Models can be defined with a minimum ensemble of free parameters which are able to *reproduce* nuclear and electron spin resonance spectra, optical spectroscopies results like fluorescence emission resolved in time, optical Kerr effect, light scattering, neutron scattering, dielectric relaxation, and many other experimental observables. Moreover, stochastic models based on multidimensional Fokker–Planck or Smoluchowski operators, once the potential energy of the augmented system solute plus solvent has been defined, are in principle able to describe the time evolution of the system in an exact way, and they also allow to *interpret* complex dynamical behaviours as combinations or superpositions of subsets of coordinates, and to discard irrelevant variables, when their relaxation is too fast or too slow in the timescale of interest.

This work is concerned with the definition, treatment and application to cases of interests of several stochastic models, in attempt to review the most recent, state-of-art results in this research area.

First, applications of standard Fokker–Planck equations for the orientational relaxation of molecules in isotropic and ordered liquid phase are reviewed. In particular attention will be focused on the interpretation of quasi-elastic neutron neutron scattering (QENS) experiments in nematics. No secondary variables or solvent degrees of freedom are included in this model, but the intrinsic complexity of the experimental QENS is shown to be captured by the treatment, by including inertial effects and anisotropy.

An extended stochastic model is used to interpret time-domain resolved fluorescence emission experiments. A two-body stochastic model allows the theoretical interpretation of dynamical Stokes shift effects in fluorescence emission spectra, performed on probes in isotropic and ordered polar phases. The system under scrutiny is assimilated to a rigid dipole rotating in a nematic phase, characterized by a set of Euler angles describing the instantaneous orientation, and coupled to the stochastic reaction field generated by the polar medium. This treatment has the advantage of directly relating the theoretical interpretation with macroscopical parameters such as the dielectric constants and the viscosity of the liquid crystal medium.

Finally, even for the case of isotropic fluids made of small molecules, a clear separation of time-scales between the relaxation of the solvent (or 'cage') structure, and the motions of the single confined molecules, has been evidenced by molecular dynamics studies. A sophisticated model, which includes as basic ingredients a Fokker–Planck description of the single molecule rotational motion and the slow diffusive motion of a persistent cage structure plus the decay processes related to the changing structure of the cage, is defined and solved numerically and analytically, and applied to the interpretation of the complex mix of orientational and librational relaxation phenomena of a typical optical Kerr effect (OKE) experiment.

The paper is organized as follows. In the next Section a general description of different stochastic models is provided, to illustrate existing formal and physical relations. In Section 3 the application of a rotational Fokker–Planck model to QENS experiments in isotropic and ordered liquid phases is presented and discussed. Section 4 is devoted to the interpretation of time resolved fluorescence emission in polar liquids, with inclusion of an orienting mean field to mimic a nematic phase. Finally Section 5 describes a more advanced treatment for isotropic fluids only, which tries to take into account as completely as possible all the elementary relaxation processes related to the set up and decay of solvent structures around a rotating probe molecule.

2. Extended stochastic models

We shall first discuss the choice of the set of stochastic variables which constitute an approximately closed Markovian space. The precise definition of the stochastic model required for interpreting a given set of experimental observations is strongly dependent of the time-window of the spectroscopical technique and the nature of the liquid phase. A general and complete *ab initio* definition of all possible stochastic treatment is an unrealistic task, equivalent, in a sense, to the full comprehension at a microscopic level of *all* the possible relaxation phenomena taking place in a liquid. We shall consider in the following only cases of coupling of local solvent structures

to the motion of a single rigid molecule, which will be referred to as probe or solute, and neglect the interference of low-frequency or hydro-dynamical modes. Our main analysis will be centered on rotational motions, since they are of great importance for the interpretation of most dynamical data obtained in liquid phases. The Fokker–Planck model for a rigid rotator assumes that the environment is responsible for the presence of white-noise forces providing a dissipative relaxation mechanism, which is superimposed to the inertial (conservative) motion of the rigid body, described by a classic Liouville operator. By neglecting the relaxation of the conjugate angular momentum (which is done only in the condition of high friction) a purely diffusive dynamics is obtained for the system, according to the standard Smoluchowski picture.

Let us consider the case of a fluid made of rigid molecules, which may carry a permanent electric dipole, and interact via short range steric interactions which may give rise to anisotropic (nematic) phases. The motion of a generic molecule is superimposed to the overall motion of a local cluster or cage of companions molecule. The cage dynamics itself is rather complex and is described at best by a mixed motion which is part small step diffusion and part strong collision motion: the former being due to the small reorientational steps that are taken by the cluster when it moves as a whole, and the latter resulting from instantaneous changes in the set of molecules forming the cluster, which enter and leave the cluster randomly. As a consequence of the first kind of motion, only the orientation of principal axis of the cage is changed; the second kind affects both the orientation of the cage and its 'internal' structure. It is possible to recover the Fokker–Planck description as a particular case of the cage model, by neglecting the coupling with the cage structure, and a two-body Smoluchowski model by considering the diffusive regime only (fast decay of the momentum) of the probe, and discarding the instantaneous changes in structure of the cage. The simplest stochastic model, *i.e.* a one-body Smoluchowski model, is obtained directly from the Fokker–Planck picture by projecting, as fast variables, the components of the probe angular momentum, or from the two-body Smoluchowski description by neglecting coupling with the cage.

2.1. The cage model

The following hypothesis are made to select the stochastic variables and to define the static and dynamic property of the system:

1. a generic molecule (probe) is represented as a rigid rotating body, with axial symmetry; either a rigid top with cylindrical symmetry of the inertia tensor or a rigid needle; the translational degrees of freedom of the probe are neglected, as they are considered essentially uncoupled to the rotational motion;

2. the local environment is made by a cluster of molecules behaving as a diffusive rigid body, which can be subjected to random changes in its internal structure;

3. the interaction potential between probe and cage is made up of two parts: a term responsible for local confined reorientations of the probe in the cage, and a term which is essentially the usual mean field term dictating the preferential orientation of the probe with respect to the external director, in the case of anisotropic phases;

4. an additional set of variables, represented by a vector $\boldsymbol{R}$ is included into the relevant set of coordinates to describe the local polarization of the solvent; a one-dimensional polarization variable was used recently to treat the solvent dynamics of an isotropic polar environment, coupled to an emitting probe with an internal degree of freedom [1]: here we use a vector description of the solvent polarization to take into account solvent effects on the full dimensionality of the rotational motion of the probe.

The polar solvent dynamics is described by the stochastic reaction field resulting by an Onsager cavity with the dielectric properties of the bulk solvent. An advantage of this phenomenological approach is the immediate relation established with the macroscopical dielectric properties of the medium, *i.e.* the dielectric tensor constants $\boldsymbol{\varepsilon}_0$ and $\boldsymbol{\varepsilon}_\infty$. A minor complication arises from the intrinsic anisotropy of the solvent, at least in the ordered phase [5].

The stochastic variables of the system are then written as:

$$\boldsymbol{Y} = (\boldsymbol{\Omega}_{\mathrm{o}}, \boldsymbol{L}, \boldsymbol{\Omega}_{\mathrm{c}}, \omega, \boldsymbol{R})\,, \tag{1}$$

where $\boldsymbol{\Omega}_{\mathrm{o}}$ are the the Euler angles giving the orientation of the probe with respect to the director; $\boldsymbol{\Omega}_{\mathrm{c}}$ are the same quantities for the cage; $\boldsymbol{L}$ is the conjugate momentum associate to $\boldsymbol{\Omega}_{\mathrm{o}}$. The quantity ω is the principal frequency of librations of the probe with respect to the cage, for molecular rotations about the x and y axis of the cage frame.

The system potential energy is written, by including only the *even* leading terms with respect to the ranks of Wigner functions in $\boldsymbol{\Omega}_{\mathrm{o}}$, and $\boldsymbol{\Omega} = \boldsymbol{\Omega}_{\mathrm{o}} - \boldsymbol{\Omega}_{\mathrm{c}}$ which represents the relative orientation of the probe with respect to the cage, in the following form:

$$V(\boldsymbol{\Omega}_{\mathrm{c}}, \boldsymbol{\Omega}_{\mathrm{o}}, \omega, \boldsymbol{R}) = V_{\mathrm{mf}}(\boldsymbol{\Omega}_{\mathrm{o}}) + V_{\mathrm{c}}(\boldsymbol{\Omega}, \omega) + V_{\mathrm{E}}(\boldsymbol{\Omega}_{\mathrm{o}}, \boldsymbol{R})\,. \tag{2}$$

The mean field term is simply written as:

$$V_{\mathrm{mf}}(\boldsymbol{\Omega}_{\mathrm{o}}) = -I_{\perp}\Omega^2\mathcal{D}^2_{0,0}(\boldsymbol{\Omega}_{\mathrm{o}})/3 \equiv -\gamma\mathcal{D}^2_{0,0}(\boldsymbol{\Omega}_{\mathrm{o}})\,, \tag{3}$$

while the probe-cage interaction term is written analogously:

$$V_{\rm c}(\boldsymbol{\Omega},\boldsymbol{\omega}) = -I_{\perp}\omega^2\mathcal{D}^2_{0,0}(\boldsymbol{\Omega})/3\,. \tag{4}$$

The electrostatic term, V_E, should accounts for the interaction between the electric dipole of the molecule and the reaction field. Finite amplitude fluctuations are imposed to the solvent polarization via a quadratic potential in $\boldsymbol{R}$ [6]:

$$V_{\rm E}(\boldsymbol{\Omega}_{\rm o},\boldsymbol{R}) = -\frac{1}{2}\boldsymbol{\mu}\boldsymbol{F}_{\infty}\boldsymbol{\mu} - \boldsymbol{\mu}\boldsymbol{R} + \frac{1}{2}\boldsymbol{R}\boldsymbol{F}^{-1}_{\rm or}\boldsymbol{R}\,, \tag{5}$$

where $\boldsymbol{\mu}$ is the electric dipole moment, depending on the orientation if expressed in the laboratory frame.

Tensors $\boldsymbol{F}_{\infty}$ and $\boldsymbol{F}_{\rm or} = \boldsymbol{F}_0 - \boldsymbol{F}_{\infty}$ are given in terms of the dielectric tensors $\boldsymbol{\varepsilon}_{\infty}$ and $\boldsymbol{\varepsilon}_0$, which are diagonal in the LF, and of the electrostatic depolarization tensors $\boldsymbol{n}$ and $\boldsymbol{n}'$, defined respectively for the cavity and *in vacuo*. A detailed derivation is presented in the Appendix. By choosing a cavity of spherical shape with radius a, one can show that for a cylindrically symmetric dielectric tensor $\boldsymbol{\varepsilon}$ (*i.e.* $\varepsilon_1 = \varepsilon_2 = \varepsilon_{\perp}$ and $\varepsilon_3 = \varepsilon_{\parallel}$), the generic $\boldsymbol{F}$ tensor is diagonal in the LF, with principal values:

$$F_1 = F_2 \;=\; F_{\perp} = \frac{1}{4\pi a^3\varepsilon_0}\frac{(1-n'_{\perp})\varepsilon_{\perp} - 2n'_{\perp}}{\varepsilon_{\perp} - n'_{\perp}(\varepsilon_{\perp}-1)} \tag{6}$$

$$F_3 \;=\; F_{\parallel} = \frac{1}{4\pi a^3\varepsilon_0}\frac{(1-n'_{\parallel})\varepsilon_{\parallel} - 2n'_{\parallel}}{\varepsilon_{\parallel} - n'_{\parallel}(\varepsilon_{\parallel}-1)}\,, \tag{7}$$

where the electrostatic depolarization tensor is:

$$n'_{\perp} \;=\; \frac{1}{2}\int_0^{\infty} dz \frac{1}{(1+z)^2[1+(\varepsilon_{\parallel}/\varepsilon_{\perp})z]^{1/2}} \tag{8}$$

$$n'_{\parallel} \;=\; \frac{1}{2}\int_0^{\infty} dz \frac{1}{(1+z)^{3/2}[1+(\varepsilon_{\perp}/\varepsilon_{\parallel})z]}\,. \tag{9}$$

$$\tag{10}$$

The principal values of $\boldsymbol{F}_0$ and $\boldsymbol{F}_{\infty}$ are obtained substituting the components of $\boldsymbol{\varepsilon}_0$ and $\boldsymbol{\varepsilon}_{\infty}$ in the previous set of equations.

The equilibrium distribution for the system is then given by:

$$P(\boldsymbol{Y}) = \frac{\exp\{-[\boldsymbol{L}^{\rm tr}\boldsymbol{I}^{-1}\boldsymbol{L}/2 + V(\boldsymbol{\Omega}_{\rm c},\boldsymbol{\Omega}_{\rm o},\omega,\boldsymbol{R})]/k_BT\}P(\omega)}{2\pi k_BTI_{\perp}\sqrt{2\pi k_BTI_{\parallel}}\int\int\int d\boldsymbol{\Omega}_{\rm o}d\boldsymbol{\Omega}_{\rm c}d\boldsymbol{R}\exp\{-V(\boldsymbol{\Omega}_{\rm c},\boldsymbol{\Omega}_{\rm o},\omega,\boldsymbol{R})/k_BT\}}. \tag{11}$$

Here $\boldsymbol{I}$ is the inertia tensor of the probe, with principal components $I_\perp$ and $I_\parallel$, and $P(\omega)$ is the reduced distribution on the librational frequency ω, which has to be defined; a simple Gaussian form was already used in recent works [2] concerning isotropic phases, although other functions are possible:

$$P(\omega) = \exp[-(\omega - \overline{\omega})^2/2\sigma_\omega^2]/\sqrt{2\pi\sigma_\omega^2}\,. \tag{12}$$

The time evolution operator is now specified according to the idea that the system $\boldsymbol{Y}$ constitutes a closed Markovian space whose temporal evolution is dictated by single elementary processes represented by Fokker–Planck or diffusive terms. The non-equilibrium distribution is obtained from the solution of the general equation:

$$\partial P(\boldsymbol{Y},t)/\partial t = -\hat{\Gamma} P(\boldsymbol{Y},t)\,. \tag{13}$$

First we divide the time evolution operator into a solute related part and solvent terms:

$$\hat{\Gamma} = \hat{\Gamma}_{\text{solute}} + \hat{\Gamma}_{\text{cage}} + \hat{\Gamma}_{\text{S}}\,. \tag{14}$$

The first term contains the operator related to rotation of the probe, *i.e.* the Fokker–Planck operator

$$\hat{\Gamma}_{\text{solute}} = \boldsymbol{L}^{\text{tr}}\boldsymbol{I}^{-1}\hat{\boldsymbol{M}}(\boldsymbol{\Omega}_{\text{o}}) + (\boldsymbol{T}+\boldsymbol{P})^{\text{tr}}\frac{\partial}{\partial \boldsymbol{L}} - k_B T\left(\frac{\partial}{\partial \boldsymbol{L}}\right)^{\text{tr}}\boldsymbol{\xi} P(\boldsymbol{Y})\left(\frac{\partial}{\partial \boldsymbol{L}}\right)P(\boldsymbol{Y})^{-1}, \tag{15}$$

where $\hat{\boldsymbol{M}}(\boldsymbol{\Omega}_{\text{o}})$ is the rotation operator acting on $\boldsymbol{\Omega}_{\text{o}}$ with components in the molecular frame.

Eq. (15) depends upon the friction tensor $\boldsymbol{\xi}$, which is diagonal, with principal components $\xi_\perp$ and $\xi_\parallel$, in the molecular frame; $\boldsymbol{T} = -\hat{\boldsymbol{M}}(\boldsymbol{\Omega}_{\text{o}})V$ is the torque vector. The precessional torque $\boldsymbol{P}$ is written explicitly as:

$$\boldsymbol{P} = \boldsymbol{L}_\times \boldsymbol{I}^{-1}\boldsymbol{L}\,, \tag{16}$$

and $\boldsymbol{L}_\times$ is a matrix such that $\boldsymbol{L}_\times \boldsymbol{v} = \boldsymbol{L} \wedge \boldsymbol{v}$ for all vectors $\boldsymbol{v}$. The precessional contribution to the streaming part of the Fokker–Planck operator is a consequence of the choise of writing the operator in the molecular system of axes. Precessional effects are null for the case of isotropic inertial tensor ($I_\perp = I_\parallel$).

Next we specify the dynamics of the cage by considering two independent processes: i) the cage rotation which does not modify the librational frequencies, and ii) the cage restructuring which randomize both the librational frequencies and the cage orientation

$$\hat{\Gamma}_{\text{cage}} = \hat{\Gamma}_{\text{cage rot.}} + \hat{\Gamma}_{\text{cage rest.}} \tag{17}$$

For the former dynamical process, a simple rotational diffusion operator will be employed

$$\hat{\Gamma}_{\text{cage rot.}} = -\hat{\boldsymbol{M}}(\boldsymbol{\Omega}_{\text{c}})^{\text{tr}}\boldsymbol{D}P(\boldsymbol{Y})\hat{\boldsymbol{M}}(\boldsymbol{\Omega}_{\text{c}})P(\boldsymbol{Y})^{-1}\,, \tag{18}$$

where $\hat{\boldsymbol{M}}(\boldsymbol{\Omega}_{\text{c}})$ is the rotation operator acting on the Euler angles $\boldsymbol{\Omega}_{\text{c}}$ and with Cartesian components in the cage frame. It is given by the same form of $\hat{\boldsymbol{M}}(\boldsymbol{\Omega}_{\text{o}})$ after substitution of $\boldsymbol{\Omega}_{\text{o}}$ with $\boldsymbol{\Omega}_{\text{c}}$. An scalar diffusion tensor will be used for simplicity in all the applications presented in this work, thus assuming that the diffusional rotation of the cage is essentially isotropic

$$\boldsymbol{D} = D\boldsymbol{1}\,. \tag{19}$$

The cage restructuring operator is built in the form of an integro-differential term, *i.e.* as a master equation which specify the rate of interchange between two given configuration $\boldsymbol{Y}$ and $\boldsymbol{Y}'$: this rate, w is the only parameter of the cage restructuring process, and the case $w \to 0$ corresponds to absence of restructuring, *i.e.* a rigid cage. The explicit form of the cage restructuring operator has been defined elsewhere [4] for a linear rotator in an isotropic medium and can defined essentially along the same lines for a rotating non-linear molecule in an anisotropic medium, *i.e.* as a master equation which specify the rate w of interchange between two given configuration $\boldsymbol{Y}$ and $\boldsymbol{Y}'$:

$$\hat{\Gamma}_{\text{cage rest.}}\; P(\boldsymbol{Y},t) = \int d\boldsymbol{Y}'[P(\boldsymbol{Y},t)W(\boldsymbol{Y}\to\boldsymbol{Y}') - P(\boldsymbol{Y}',t)W(\boldsymbol{Y}'\to\boldsymbol{Y})]\,, \tag{20}$$

with a transition kernel $W(\boldsymbol{Y}\to\boldsymbol{Y}')$ dependent in general on the initial configuration $\boldsymbol{Y}$ and the final one $\boldsymbol{Y}'$. Two constraints are imposed for choosing the transition kernel: the detailed balance condition and the condition that instantaneous changes of the solvent cage do not modify the solute configuration, *i.e.* that the $(\boldsymbol{\Omega}_{\text{o}}, \boldsymbol{L})$ variables remain constant during cage restructuring. Correspondingly we choose a BGK [7] rate kernel with respect to the solvent (cage and reaction field) variables only:

$$W(\boldsymbol{Y}\to\boldsymbol{Y}') = \mathcal{W}(\boldsymbol{\Omega}_{\text{c}} - \boldsymbol{\Omega}'_{\text{c}})\delta(\boldsymbol{\Omega}'_{\text{o}} - \boldsymbol{\Omega}_{\text{o}})\delta(\boldsymbol{L}' - \boldsymbol{L})P(\boldsymbol{\Omega}', \omega', \boldsymbol{R}')\,, \tag{21}$$

where $P(\boldsymbol{\Omega}', \omega', \boldsymbol{R}')$ is the equilibrium distribution of the solvent variables in the arrival state for a given solute orientation, *i.e.* the Boltzmann distribution with respect to $V(\boldsymbol{\Omega}', \omega', \boldsymbol{R}')$ multiplied by $P(\omega')$. A function $\mathcal{W}(\boldsymbol{\Omega}_{\text{c}} - \boldsymbol{\Omega}'_{\text{c}})$ has to be introduced in order to control the distribution in size of the cage reorientations. The effective rate w can be assigned to the cage restructuration processes on the basis of the average decay rate of all cage structures

$$w = \int d\boldsymbol{Y}d\boldsymbol{Y}'P(\boldsymbol{Y})W(\boldsymbol{Y}\to\boldsymbol{Y}')\,. \tag{22}$$

The term responsible for the relaxation of solvent polarisation is also assumed to be diffusive in nature and it is represented by a Smoluchowski operator:

$$\hat{\Gamma}_{\mathrm{S}} = -\left(\frac{\partial}{\partial \boldsymbol{R}}\right)^{\mathrm{tr}} \boldsymbol{D}_S P(\boldsymbol{Y}) \left(\frac{\partial}{\partial \boldsymbol{R}}\right) P(\boldsymbol{Y})^{-1}, \tag{23}$$

where the diffusion tensor $\boldsymbol{D}_S$ is given in terms of the solvent relaxation times:

$$\boldsymbol{D}_S/k_BT = \begin{pmatrix} F_{\mathrm{or}}^{\perp}/\tau_S^{\perp} & 0 & 0 \\ 0 & F_{\mathrm{or}}^{\perp}/\tau_S^{\perp} & 0 \\ 0 & 0 & F_{\mathrm{or}}^{\parallel}/\tau_S^{\parallel} \end{pmatrix}. \tag{24}$$

The model is completely defined by the following parameters: the streaming frequencies $\omega_s^{\perp,\parallel} = \sqrt{k_BT/I^{\perp,\parallel}}$, the average librational frequency $\overline{\omega}$, the distribution width σ_ω and the mean field frequency Ω. Dynamic parameters, characterizing the rates of dissipation associated with the relaxation processes, are the collision times $\tau_{\mathrm{c}}^{\perp,\parallel} = I^{\perp,\parallel}/\xi^{\perp,\parallel}$, the cage diffusion coefficient D and the rate of cage restructuring w. Finally polar static effects are parameterized by tensors $\boldsymbol{F}_\infty$ and $\boldsymbol{F}_{\mathrm{or}}$, *i.e.* essentially by the dielectric constants; and dynamical polar solvent effects by $\tau_S^{\perp}$ and $\tau_S^{\parallel}$, which can be in turn connected to Debye relaxation times. A compact representation of the operator is obtained after defining the overall gradient with respect to all variables, minus the frequency of restructuring of the cage:

$$\hat{\boldsymbol{\nabla}}_{\boldsymbol{Y}} = \begin{pmatrix} \hat{\boldsymbol{M}}(\boldsymbol{\Omega}_{\mathrm{o}}) \\ \dfrac{\partial}{\partial \boldsymbol{L}} \\ \hat{\boldsymbol{M}}(\boldsymbol{\Omega}_{\mathrm{c}}) \\ \dfrac{\partial}{\partial \boldsymbol{R}} \end{pmatrix}. \tag{25}$$

The operator can then be written in the form:

$$\begin{aligned} \hat{\Gamma} &= \hat{\Gamma}_{\mathrm{solute}} + \hat{\Gamma}_{\mathrm{cage\ rot.}} + \hat{\Gamma}_{\mathrm{S}} + \hat{\Gamma}_{\mathrm{cage\ rest.}} \\ &= -\hat{\boldsymbol{\nabla}}_{\boldsymbol{Y}}^{\mathrm{tr}} \boldsymbol{a}_{\boldsymbol{Y}} P(\boldsymbol{Y}) \hat{\boldsymbol{\nabla}}_{\boldsymbol{Y}} P(\boldsymbol{Y})^{-1} + \hat{\Gamma}_{\mathrm{cage\ rest.}}, \end{aligned} \tag{26}$$

where $\boldsymbol{a}_{\boldsymbol{Y}}$ is the matrix:

$$\boldsymbol{a}_{\boldsymbol{Y}} = \begin{pmatrix} \boldsymbol{0} & -k_BT\boldsymbol{1} & \boldsymbol{0} & \boldsymbol{0} \\ k_BT\boldsymbol{1} & k_BT(\boldsymbol{\xi} - \boldsymbol{L}_\times) & \boldsymbol{0} & \boldsymbol{0} \\ \boldsymbol{0} & \boldsymbol{0} & D\boldsymbol{1} & \boldsymbol{0} \\ \boldsymbol{0} & \boldsymbol{0} & \boldsymbol{0} & \boldsymbol{D}_S \end{pmatrix}. \tag{27}$$

2.2. Fokker–Planck model

We are now able to underline the formal relations which exist with previous stochastic models. Let us consider the Fokker–Planck model (FP). By assuming that the probe is much larger than the solvent particles, we may consider that the coupling of the cage structure with the probe itself is rather weak: for a massive probe immersed in a fluid of microscopic particles, the cage structure looses meaning. Thus coupling with $\boldsymbol{\Omega}_{\mathrm{c}}$ and ω is neglected. Also, if non polar molecules are considered, the coupling with the reaction field or solvent polarisation disappears For a generic function depending only upon the probe coordinates, $f(\boldsymbol{\Omega}_{\mathrm{o}}, \boldsymbol{L})$, the time evolution operator is obtained in the standard Fokker–Planck form:

$$\hat{\Gamma}_{\mathrm{FP}} = \boldsymbol{L}^{\mathrm{tr}} \boldsymbol{I}^{-1} \hat{\boldsymbol{M}}(\boldsymbol{\Omega}_{\mathrm{o}}) + (\boldsymbol{T}+\boldsymbol{P})^{\mathrm{tr}} \frac{\partial}{\partial \boldsymbol{L}} - k_B T \left(\frac{\partial}{\partial \boldsymbol{L}}\right)^{\mathrm{tr}} \boldsymbol{\xi} P(\boldsymbol{\Omega}_{\mathrm{o}}, \boldsymbol{L}) \left(\frac{\partial}{\partial \boldsymbol{L}}\right) P(\boldsymbol{\Omega}_{\mathrm{o}}, \boldsymbol{L})^{-1}, \tag{28}$$

which is naturally equivalent to $\hat{\Gamma}_{\mathrm{solute}}$, defined with respect to a potential which includes only V_{mf}.

2.3. Smoluchowski models

The standard Smoluchowski model (S) is immediately recovered from the FP model under the well-known condition of fast relaxation of the probe momentum components; this condition can be formally expressed in terms of collisional times and streaming frequencies by assuming that:

$$\tau_{\mathrm{c}}^{\perp,\parallel} << 1/\omega_s^{\perp,\parallel}, \tag{29}$$

i.e. the perpendicular and parallel collision times must be very small compared to the time scale of the conservative motions. A straightforward projection is performed with respect to the fast variables $\boldsymbol{L}$ and a standard Smoluchowski operator is obtained:

$$\hat{\Gamma}_{\mathrm{S}} = -\hat{\boldsymbol{M}}(\boldsymbol{\Omega}_{\mathrm{o}})^{\mathrm{tr}} \boldsymbol{D}_R P(\boldsymbol{\Omega}_{\mathrm{o}}) \hat{\boldsymbol{M}}(\boldsymbol{\Omega}_{\mathrm{o}}) P(\boldsymbol{\Omega}_{\mathrm{o}})^{-1}, \tag{30}$$

where $P(\boldsymbol{\Omega}_{\mathrm{o}}) = \int d\boldsymbol{L} P(\boldsymbol{\Omega}_{\mathrm{o}}, \boldsymbol{L})$ is the Boltzmann distribution with respect to the mean field potential only and where the effective diffusion tensor, diagonal in the molecular frame, has the principal components:

$$D_R^{\perp,\parallel} = {\omega_s^{\perp,\parallel}}^2 \tau_{\mathrm{c}}^{\perp,\parallel}. \tag{31}$$

A two-body Smoluchowski model (S2) can be considered, when *(i)* probe inertial motions are negligible, *(ii)* no polar static and dynamical effects are taken into account, *(iii)* cage restructuring is neglected. The time evolution operator obtained in this case is

$$\begin{aligned} \hat{\Gamma}_{\mathrm{S2}} = & - \hat{\boldsymbol{M}}(\boldsymbol{\Omega}_{\mathrm{o}})^{\mathrm{tr}} \boldsymbol{D}_R P(\boldsymbol{\Omega}_{\mathrm{o}}, \boldsymbol{\Omega}_{\mathrm{c}}) \hat{\boldsymbol{M}}(\boldsymbol{\Omega}_{\mathrm{o}}) P(\boldsymbol{\Omega}_{\mathrm{o}}, \boldsymbol{\Omega}_{\mathrm{c}})^{-1} \\ & - D \hat{\boldsymbol{M}}(\boldsymbol{\Omega}_{\mathrm{c}})^{\mathrm{tr}} P(\boldsymbol{\Omega}_{\mathrm{o}}, \boldsymbol{\Omega}_{\mathrm{c}}) \hat{\boldsymbol{M}}(\boldsymbol{\Omega}_{\mathrm{c}}) P(\boldsymbol{\Omega}_{\mathrm{o}}, \boldsymbol{\Omega}_{\mathrm{c}})^{-1}, \end{aligned} \tag{32}$$

i.e. it corresponds to the motion of two diffusive bodies coupled by the local potential $V(\boldsymbol{\Omega}_{\rm o}-\boldsymbol{\Omega}_{\rm c})$ with axially symmetric diffusion tensor ($D_R^{\perp}$ and $D_R^{\parallel}$) for the probe, and the isotropic diffusion coefficient D for the cage. This model has been extensively used in the interpretation of ESR spectra of paramagnetic probes in liquid crystals [8]and glassy fluids [9].

Finally, a Smoluchowski model (SS) which includes the probe orientation and the polarization field as principal stochastic variable is obtained by retaining only the relaxation and static terms pertaining to $\boldsymbol{\Omega}_{\rm o}$ and $\boldsymbol{R}$:

$$\begin{aligned}\hat{\Gamma}_{\rm SS} = & - \hat{\boldsymbol{M}}(\boldsymbol{\Omega}_{\rm o})^{\rm tr}\boldsymbol{D}_R P(\boldsymbol{\Omega}_{\rm o},\boldsymbol{R})\hat{\boldsymbol{M}}(\boldsymbol{\Omega}_{\rm o})P(\boldsymbol{\Omega}_{\rm o},\boldsymbol{R})^{-1} \\ & - \left(\frac{\partial}{\partial \boldsymbol{R}}\right)^{\rm tr}\boldsymbol{D}_S P(\boldsymbol{\Omega}_{\rm o},\boldsymbol{R})\left(\frac{\partial}{\partial \boldsymbol{R}}\right)P(\boldsymbol{\Omega}_{\rm o},\boldsymbol{R})^{-1}\,. \end{aligned} \tag{33}$$

This model has been used to rationalize time resolved fluorescence emission spectra of large rotating probes in polar isotropic and nematic phases [10,11].

2.4. Numerical solution

The usefulness of stochastic models can be limited if an efficient technique to extract the necessary information, *i.e.* to calculate explicitly the correlation functions of interests and their dependence upon the parameters, is not available. When relatively large phase space of variables are considered, tools to accomplish this task are lacking. However, very efficient procedures can be applied to rather complex problems by combining the projection of the time evolution operator in a functional space of functions, either orthogonal or non-orthogonal, and a treatment of the resulting and highly effective iterative techniques on sparse matrices like the Lanczos algorithm. Efficient approximate techniques are also available which are based upon the separation of timescales among different subsets of variables.

In general, the first step to solve numerically a stochastic model is to choose a suitable set of basis functions $|N\rangle$, which is usually defined as the direct product of sets of functions defined for the coordinates or groups of them. The collective index N identifies completely each member of the basis set. The superposition matrix $\boldsymbol{S}$, with elements

$$S_{N,N'} \equiv \langle N|N'\rangle \tag{34}$$

is eventually required to account for the non-orthogonality of the basis set. Once the basis functions are chosen, the matrix representation must be generated for a generic correlation function of two observables $f(\boldsymbol{Y})$ and $g(\boldsymbol{Y})$ given as linear combinations of the basis elements

$$f(\boldsymbol{Y})P(\boldsymbol{Y})^{1/2} = \sum_N f_N|N\rangle \qquad g(\boldsymbol{Y})P(\boldsymbol{Y})^{1/2} = \sum_N g_N|N\rangle\,. \tag{35}$$

Let us consider the correlation function in the symmetrized form

$$G(t) = \langle f| \exp(-\hat{\Gamma} t)|gP\rangle = \langle fP^{1/2}| \exp(-\tilde{\Gamma} t)|gP^{1/2}\rangle \tag{36}$$

defined with respect to the symmetrized time evolution operator

$$\tilde{\Gamma} \equiv P(\boldsymbol{Y})^{-1/2} \hat{\Gamma} P(\boldsymbol{Y})^{1/2} \,. \tag{37}$$

Actual calculations are necessarily performed with a truncated set of basis elements, and this is equivalent to substitute the full correlation function with a projected counterpart

$$G(t) = \langle fP^{1/2}| \exp(-\tilde{\Gamma}\hat{\mathcal{P}} t)|gP^{1/2}\rangle \,, \tag{38}$$

$\hat{\mathcal{P}}$ being the projection operator onto the subspace spanned by the truncated basis set

$$\hat{\mathcal{P}} = \sum_{N,N'} |N\rangle (\boldsymbol{S}^{-1})_{N,N'} \langle N'| \,, \tag{39}$$

with the summations restricted to the allowed values of indexes N and N'. By expanding in Taylor series the exponential term

$$\begin{aligned} G(t) &= \sum_k \frac{(-t)^k}{k!} \langle fP^{1/2}| (\tilde{\Gamma}\hat{\mathcal{P}})^k |P^{1/2} g\rangle = \sum_k \frac{(-t)^k}{k!} \boldsymbol{f}^\dagger (\boldsymbol{\Gamma}\boldsymbol{S}^{-1})^k \boldsymbol{S}\boldsymbol{g} \\ &= \boldsymbol{f}^\dagger \exp(-\boldsymbol{\Gamma}\boldsymbol{S}^{-1} t) \boldsymbol{S}\boldsymbol{g} \end{aligned} \tag{40}$$

one recovers the matrix form of the correlation function to be evaluated with the methods of linear algebra. The coefficients of expansions (35) are collected in the arrays $\boldsymbol{f}$ and $\boldsymbol{g}$, while $\boldsymbol{\Gamma}$ is the matrix representation of the evolution operator

$$\Gamma_{N,N'} = \langle N|\tilde{\Gamma}|N'\rangle \,. \tag{41}$$

Because of the lack of symmetry in the matrix $\boldsymbol{\Gamma}\boldsymbol{S}^{-1}$, we can employ the Lanczos algorithm for symmetric or non-symmetric matrices which generates iteratively an orthogonal or bi-orthogonal basis, respectively. The required number of iterations is typically much smaller than the matrix dimension.

3. Interpretation of quasi-elastic neutron scattering in liquids

The autocorrelation function of a generic observable f is defined as:

$$G(t) = \overline{f(0) f(t)} = \langle f| \exp(-\hat{\Gamma} t)|fP\rangle \tag{42}$$

being $\hat{\Gamma}$ the time evolution operator for the variables whose dynamics has been retained either because f depends directly upon them (primary variables), or because they are associated to the primary variables (momenta,

cage variables, polarisation vectors and so on): P is the Boltzmann distribution. The time Fourier transform is defined as

$$S(\omega) = \frac{1}{2\pi} \int_{-\infty}^{+\infty} dt \exp(-i\omega t) G(t) = \hat{\mathcal{F}}[G(t)] \,. \tag{43}$$

The physical observable in QENS experiments is related to the scattering function $S_s(\boldsymbol{Q}, \omega)$, where $\boldsymbol{Q}$ is the scattering vector associated to the transferred linear momentum $\hbar\boldsymbol{Q}$ and ω is the angular frequency related to the energy $\hbar\omega$ exchanged between the quasi-elastic process involving the neutron beam and the single (incoherent) scattering centre. In the following, only a single proton nucleus is considered, defined by vector $\boldsymbol{r_H}$ in the laboratory frame. The full scattering function is defined according to the following expression [12, 13]:

$$S_s(\boldsymbol{Q}, \omega) = \hat{\mathcal{F}}[I_s(\boldsymbol{Q}, t)] \,, \tag{44}$$

where $I_s(\boldsymbol{Q}, t)$ is the *intermediate scattering function*, which is the Fourier transform in the space domain of the Van Hove positional autocorrelation function for the scattering centre:

$$I_s(\boldsymbol{Q}, t) \;=\; \overline{\exp[i\boldsymbol{Q} \cdot \boldsymbol{r_H}(0)] \exp[-i\boldsymbol{Q} \cdot \boldsymbol{r_H}(t)]} \,. \tag{45}$$

3.1. Neutron scattering correlation function

In the case of slow translational dynamics, by taking into account just the rotational motions with fixed centre of mass of the probe molecule, the autocorrelation function is expanded in terms of a sum of correlation functions of Wigner rotational matrices of all ranks, weighted by factors depending upon the experimental geometry (which is defined by the vector $\boldsymbol{Q}$) and the molecular motion. For a collection of scattering centres, the additivity law holds for $S_s(\boldsymbol{Q}, \omega)$. In the case of a rod-like molecule the total scattering function be expressed in the following form by using the Rayleigh expansion of the complex exponential:

$$\begin{aligned} S_s(\boldsymbol{Q}, \omega) \;&=\; (4\pi)^2 \sum_{l_1, l_2 = 0}^{+\infty} (\imath)^{l_1} (-\imath)^{l_2} j_{l_1}(Qr_H) j_{l_2}(Qr_H) \\ &\times\; \sum_{m, m'} Y^*_{l_1 m}(\boldsymbol{\Omega_Q}^{\mathrm{L}}) Y^*_{l_1 m'}(\boldsymbol{\Omega_H}^{\mathrm{M}}) Y_{l_2 m}(\boldsymbol{\Omega_Q}^{\mathrm{L}}) Y_{l_2 m'}(\boldsymbol{\Omega_H}^{\mathrm{M}}) \\ &\times\; \hat{\mathcal{F}}\{\overline{\mathcal{D}^{l_1}_{mm'}[\boldsymbol{\Omega}_{\mathrm{o}}(0)] \mathcal{D}^{l_2}_{mm'}[\boldsymbol{\Omega}_{\mathrm{o}}(t)]}\} \,, \end{aligned} \tag{46}$$

where $\boldsymbol{\Omega_Q}^{\mathrm{L}} = (\phi_Q^{\mathrm{L}}, \theta_Q^{\mathrm{L}})$ are the angles defining the orientation of $\boldsymbol{Q}$ in the laboratory frame, and $\boldsymbol{\Omega_H}^{\mathrm{M}} = (\phi_H^{\mathrm{M}}, \theta_H^{\mathrm{M}})$ are the angles for the orientation

of the single proton, *i.e.* the incoherent scattering centre, in the molecular frame; $j_l(z)$ are Bessel spherical functions. The indexes m, m' assume all the values compatible with the rank of the spherical harmonics functions. The full scattering function can be divided in two contributes:

$$S_s(\boldsymbol{Q},\omega) = \mathrm{EISF}(\boldsymbol{Q})\delta(\omega) + S_{qe}(\boldsymbol{Q},\omega)\,, \tag{47}$$

where $\mathrm{EISF}(\boldsymbol{Q})$ is the elastic incoherent structure factor, *i.e.* the pure elastic component, and $S_{qe}(\boldsymbol{Q},\omega)$ is the quasi-elastic term which contains information about the relaxation processes. The expansion of the product of two spherical harmonics allows one to write the quasi-elastic component in the form

$$\begin{aligned} S_{qe}(\boldsymbol{Q},\omega) \;=\; & \sum_{l_1,l_2=0}^{+\infty} \sum_{m,m'} \sum_{k_1,k_2} (-1)^{m+m'} (\imath)^{l_1} (-\imath)^{l_2} [l_1 l_2] j_{l_1}(Qr_H) j_{l_2}(Qr_H) \\ & \times\; C(l_1 l_2 k_1; -m\ m) C(l_1 l_2 k_2; -m'\ m') C(l_1 l_2 k_1; 0\ 0) C(l_1 l_2 k_2; 0\ 0) \\ & \times\; \mathrm{P}_{k_1}(\cos\theta_Q^{\mathrm{L}}) \mathrm{P}_{k_2}(\cos\theta_H^{\mathrm{M}}) \\ & \times\; \hat{\mathcal{F}}\{\overline{\delta\mathcal{D}^{l_1}_{mm'}[\boldsymbol{\Omega}_{\mathrm{o}}(0)] \delta\mathcal{D}^{l_2}_{mm'}[\boldsymbol{\Omega}_{\mathrm{o}}(t)]}\}\,, \end{aligned} \tag{48}$$

where k_1, k_2 assume all the integer values between $\mid l_1 - l_2 \mid$ and $(l_1 + l_2)$; $[l_1 l_2]$ stands for $(2l_1+1)(2l_2+1)$, and $\delta\mathcal{D}^{l}_{m,m'}$ is the Wigner matrix function minus its average with respect to the Boltzmann distribution P. The elastic component $\mathrm{EISF}(\boldsymbol{Q})$ is easily obtained as :

$$\begin{aligned} \mathrm{EISF}(\boldsymbol{Q}) \;=\; & \sum_{l_1,l_2=0}^{+\infty} \imath^{l_1+l_2} [l_1 l_2] j_{l_1}(Qr_H) j_{l_2}(Qr_H) \\ & \times\; \mathrm{P}_{l_1}(\cos\theta_Q^{\mathrm{L}}) \mathrm{P}_{l_1}(\cos\theta_H^{\mathrm{M}}) \mathrm{P}_{l_2}(\cos\theta_Q^{\mathrm{L}}) \mathrm{P}_{l_2}(\cos\theta_H^{\mathrm{M}})\ \overline{\mathrm{P}_{l_1}}\ \overline{\mathrm{P}_{l_2}}\,, \end{aligned} \tag{49}$$

and $\mathrm{P}_l(\cos\theta)$ is a Legendre polynomial; $\overline{\mathrm{P}_l}$ is the order parameter of l-rank:

$$\overline{\mathrm{P}_l} \;=\; \overline{\mathrm{P}_l(\cos\beta_{\mathrm{o}})P}\,. \tag{50}$$

In expression (49) the sum is limited to l_1, l_2 assuming even values. The extension of these relations to the isotropic case is immediate.

A drastic simplifications of the previous expressions is achieved when symmetries are taken into account. Thus, the number of the independent auto-correlation functions of Wigner matrices to be calculated is largely reduced. It is interesting to note that only the autocorrelation functions, or the mixed correlation functions with l_1, l_2 both even or odd, contribute to the scattering function. Further simplified expressions can be obtained in

the case of a single scattering centre located on the long-molecular axis of probe, that is $\theta_H^{\mathrm{M}} = 0$. In this case, it is simple to demonstrate that only correlation functions $\overline{\delta\mathcal{D}^{l_1}_{m,0}[\boldsymbol{\Omega}_{\mathrm{o}}(0)]\delta\mathcal{D}^{l_2}_{m,0}[\boldsymbol{\Omega}_{\mathrm{o}}(t)]}$ have a non-zero weight. In particular, in the case of the centre placed on the long axis and $\boldsymbol{Q} \parallel \hat{\boldsymbol{z}}$ (that is parallel to the director of the uniaxial phase, in the case of a nematic liquid crystal), the relation (48) becomes :

$$S_{qe}(\boldsymbol{Q},\omega)_{\theta_H=0,\boldsymbol{Q}\parallel} = \sum_{l_1,l_2=0}^{+\infty} (\imath)^{l_1}(-\imath)^{l_2}[l_1 l_2] j_{l_1}(Qr_H) j_{l_2}(Qr_H) \times \hat{\mathcal{F}}\{\delta\mathcal{D}^{l_1}_{00}[\boldsymbol{\Omega}_{\mathrm{o}}(0)]\delta\mathcal{D}^{l_2}_{00}[\boldsymbol{\Omega}_{\mathrm{o}}(t)]\}\,. \tag{51}$$

In the case of $\boldsymbol{Q} \perp \hat{\boldsymbol{z}}$ the expression for $S_{qe}(\boldsymbol{Q},\omega)$ is more complex. In any case, a selection rule due to the intrinsic symmetries of the spherical harmonics functions for $\theta_Q^{\mathrm{L}} = \frac{\pi}{2}$ limits the correlation functions with non-null weight to those with $l_1 \neq |m|+1$ and $l_2 \neq |m|+1$.

It is interesting to investigate the behaviour of the quasi-elastic function for $\boldsymbol{Q}$ parallel and perpendicular to the director of the phase — when the centre is located on the long axis — for small arguments of the Bessel functions (approximately $Qr_H \leq 1$). In such case, the correlation functions of the first-rank Wigner functions have dominant weights upon the others. In particular, the following approximations have been numerically tested:

$$S_{qe}(\boldsymbol{Q},\omega)_{\boldsymbol{Q}\parallel} = 9\, j_1(Qr_H)^2 \hat{\mathcal{F}}\{\overline{\delta\mathcal{D}^1_{00}[\boldsymbol{\Omega}_{\mathrm{o}}(0)]\delta\mathcal{D}^1_{00}[\boldsymbol{\Omega}_{\mathrm{o}}(t)]}\}\,, \tag{52}$$

$$S_{qe}(\boldsymbol{Q},\omega)_{\boldsymbol{Q}\perp} = 9\, j_1(Qr_H)^2 \hat{\mathcal{F}}\{\overline{\delta\mathcal{D}^1_{10}[\boldsymbol{\Omega}_{\mathrm{o}}(0)]\delta\mathcal{D}^1_{10}[\boldsymbol{\Omega}_{\mathrm{o}}(t)]}\}\,. \tag{53}$$

3.2. Fokker–Planck dynamical model for neutron scattering

A standard FP model has been applied recently to the calculation of correlation functions (48) and (49), for the case of a rotating scattering centre in nematic liquid phases. Cage and solvent polarisation effects should in principle be included to achieve a better understanding of the QENS observables; however, the additional complexity in the neutron scattering interpretation — the signal is always linked to complicate combinations of many orientational correlation functions — and the difficulties in the analysis of the experimental data suggest the opportunity of considering standard models, before attacking the problem of solvent static and dynamical effects. The following analysis is then based on the exact numerical exploration of the FP only because this model can be considered as a paradigmatic interpretation of the rotational dynamics of a probe molecule (at least in the absence of

cage effects). The results presented here have been selected with the purpose of showing that the model is sensitive to geometric (orientation of vector $\boldsymbol{Q}$), frictional (collisional times, *i.e.* probe friction tensor) and phase-related (mean-field potential) parameters. Actual comparison between experimental observations and model simulation are currently carried on [14].

The dynamical model, *i.e.* the time evolution operator for the phase space of variables given by the Euler angles $\boldsymbol{\Omega}_{\rm o}$ and the conjugate momentum vector $\boldsymbol{L}$ is given by Eq. (28), defined with respect to the mean-field potential specified by Eq. (3). The model is then controlled by the two streaming frequencies $\omega_s^{\perp}$ and $\omega_s^{\parallel}$; by the collisional times $\tau_c^{\perp}$ and $\tau_{\rm c}^{\parallel}$; and finally by the potential strength parameter γ.

Let us now specialize the general numerical treatment described above to this particular case. We represent the FP operator in matrix form with respect to the following set of basis functions

$$\begin{aligned} |N\rangle \equiv & \left(\frac{[J_{\rm o}]}{8\pi^2}\right)^{1/2} \mathcal{D}^{J_{\rm o}}_{M_{\rm o},K_{\rm o}}(\boldsymbol{\Omega}_{\rm o})^* \\ & \times {\rm He}_{n_1}(L_1/\sqrt{k_BTI^{\perp}}){\rm He}_{n_2}(L_2/\sqrt{k_BTI^{\perp}}){\rm He}_{n_3}(L_3/\sqrt{k_BTI^{\parallel}}) \\ & \times \exp(-\boldsymbol{L}\boldsymbol{I}^{-1}\boldsymbol{L}/4k_BT)/(2\pi)^{3/4}\,. \end{aligned} \tag{54}$$

The ensemble of elementary indexes are collectively represented by N:

$$N \equiv (J_{\rm o}, M_{\rm o}, K_{\rm o}, n_1, n_2, n_3)\,. \tag{55}$$

Matrix elements are calculated analytically; explicit expressions for related or similar computational problems have been presented elsewhere [15]. Let us analyze separately the functional dependence on the different stochastic variables. For the solute orientational degrees of freedom the Wigner functions of orientation $\boldsymbol{\Omega}_{\rm o}$ have been chosen. For the angular momentum the Hermite functions of the scaled momentum vector are employed like in previous studies of the Brownian rotational motion of linear molecules. These functions are orthogonal: the general analysis is simplified since the overlap matrix is equal to the identity matrix. Matrices dimensions are rather large: truncation parameters chosen for the results presented here have been $J_{\rm o}^{\rm max} = 4-5$ and $n_i^{\rm max} = 6-7$, which correspond to dimensions of 10000-20000. Lanczos algorithm has been employed to calculate the correlation functions. We present here a few preliminary simulations, calculated for the case of a nematic with order parameter $\overline{\rm P}_2 = 0.33$, *i.e.* $\gamma = 1.5k_BT$. For the case of a spherical rotator, $\omega_s^{\perp} = \omega_s^{\parallel} = 1$ ps^{-1}, and for a cylindrical rotator, $\omega_s^{\perp} = 0.7$ ps^{-1} and $\omega_s^{\parallel} = 1.3$ ps^{-1}. In both cases the collisional times have been chosen all equal to 1 ps (isotropic friction tensor). The value of $|\boldsymbol{Q}||\boldsymbol{r}_H|$

has been fixed to 0.5 and 2 in the spherical case, and 2 in the cylindrical case. In order to show the dependence of the geometry of the scattering centre, three orientations of $\boldsymbol{Q}$ with respect to the phase director have been considered, namely 0°, 45° and 90°. Finally, the scattering centre has been always taken along the z-axis of the rotating probe. The experimental geometry is summarized in Fig. 1.

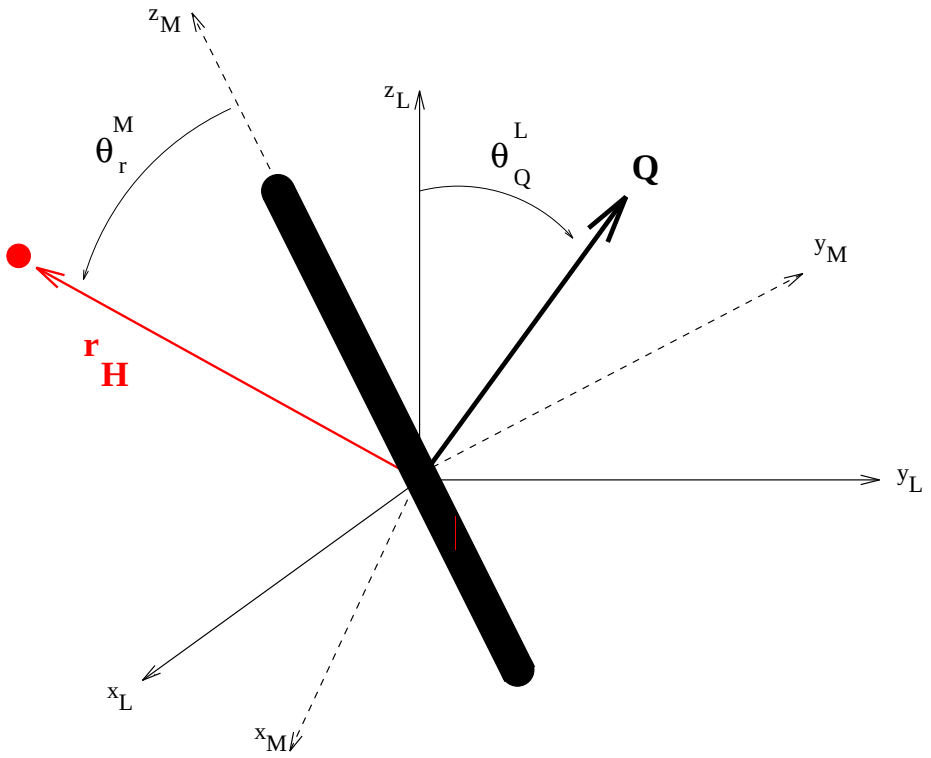

Fig. 1. Experimental geometry of a quasi-elastic neutron scattering experiment with a single scattering center.

The first set of calculated result is given in Fig. 2. The first two drawings, *(a)* and *(b)*, present S_{qe} with respect to ω for the spherical case; the third one, (*c)*, has been calculated for the cylindrical case. The simulations clearly show a strong dependence upon the angle between $\boldsymbol{Q}$ and the director, θ_Q^{L}. At intermediate values of θ_Q^{L}, the increased $|\boldsymbol{Q}||\boldsymbol{r}_H|$ parameter is responsible for lowering significantly $S_{qe}(0)$: compare *(a)* and *(b)*. The anisotropy in the inertia tensor is the cause of a further shift to higher frequencies, especially at high values of θ_Q^{L}, cfr. *(c)*. The dependence of the geometrical factor of a given rotational correlation function with respect to θ_Q^{L} can be explored

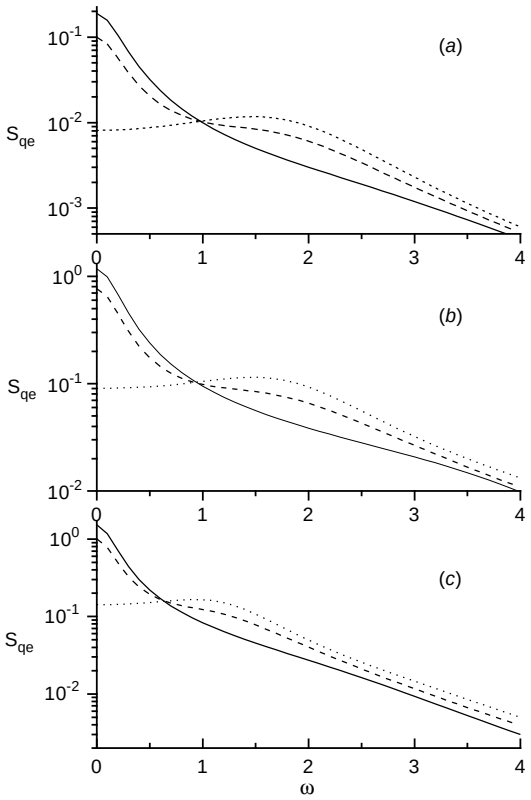

Fig. 2. Quasi-elastic component of the scattering function. Full lines: $\theta_Q^{\mathrm{L}} = 0°$; dashed lines: $\theta_Q^{\mathrm{L}} = 45°$; dotted lines: $\theta_Q^{\mathrm{L}} = 90°$. *(a)*: isotropic case, $|\boldsymbol{Q}||\boldsymbol{r}_H| = 0.5$; *(b)*: isotropic case, $|\boldsymbol{Q}||\boldsymbol{r}_H| = 2$; *(c)*: anisotropic case, $|\boldsymbol{Q}||\boldsymbol{r}_H| = 2$.

directly, by defining

$$S_s(\boldsymbol{Q},\omega) = \sum_{l_1,l_2,m,m'} \mathrm{a}(l_1,l_2,m,m')\hat{\mathcal{F}}[\overline{\mathcal{D}^{l_1}_{m,m'}(0)\mathcal{D}^{l_2}_{m,m'}(t)}]\,. \qquad (56)$$

In Fig. 3 we report as functions of θ_Q^{L} the coefficients $\mathrm{a}(1,1,0,0)$, $\mathrm{a}(1,1,1,0)$ *(a)* and $\mathrm{a}(2,2,0,0)$, $\mathrm{a}(2,2,1,0)$, $\mathrm{a}(2,2,2,0)$ *(b)*, which correspond to dominant terms, for $|\boldsymbol{Q}||\boldsymbol{r}_H| = 1$. This analysis allows to obtain approximate expressions for the scattering function by including only a few contribution, *cf.* Eqn (52) and (53). In Fig. 4, we show the exact and approximate calculated S_{qe} for $\theta_Q^{\mathrm{L}} = 0$ *(a)* and 90 *(b)*, when $|\boldsymbol{Q}||\boldsymbol{r}_H| = 1$: the agreement is better for small values of $|\boldsymbol{Q}||\boldsymbol{r}_H|$, *i.e.* small arguments of the Bessel functions which appear in the definition of the scattering function.

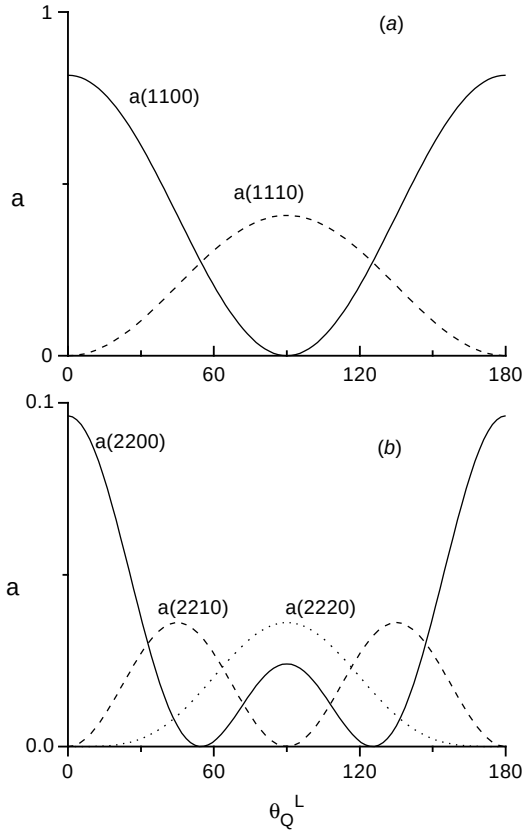

Fig. 3. Coefficients a$(1,1,0,0)$, a$(1,1,1,0)$ *(a)* and a$(2,2,0,0)$, a$(2,2,1,0)$, a$(2,2,2,0)$ *(b)*. for $|\boldsymbol{Q}||\boldsymbol{r}_H| = 1$.

4. Time resolved fluorescence in ordered phases

In this Section, we consider the case of the rotational dynamics of an electric dipole in a polar solvent, treated as a rigid diffusive rotator coupled to a vector representing the fluctuating polarization of the medium. The model has been already used recently to interpret the dynamical Stokes shift of fluorescence emission spectra obtained from rigid coumarin dyes in polar isotropic liquids and liquid crystals [10, 11]. Exact computational solutions of the full time evolution operator have been presented, and compared to measured time resolved fluorescence spectra. Here we review some of these results and we present some new conclusions concerning semi-analytical solutions which are possible when one chosen subset of variables (the rotational degrees of freedom of the emitting probe, or the vector polarization) is significantly faster than other degrees of freedom. In particular, we intend

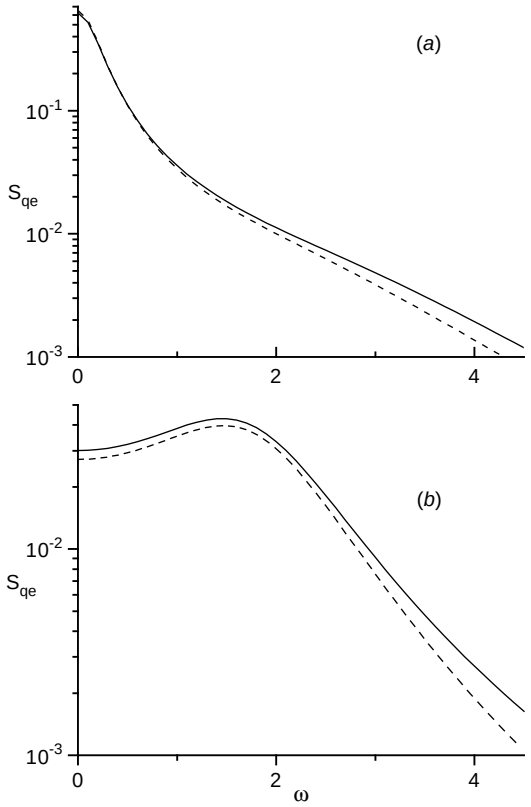

Fig. 4. Exact (full lines) and approximate (dashed lines) S_{qe} for $\theta_Q^{\mathrm{L}} = 0$ *(a)* and 90 *(b)*, for $|\boldsymbol{Q}||\boldsymbol{r}_H| = 1$.

to show that several different dynamical regimes can result by changing the anisotropy ratio, *i.e.* the ratio between the characteristic timescales of solute and solvent. Both Stokes shift time correlation functions, which are immediately related to solvation dynamics, and orientational correlation functions for the probe coordinates will be calculated and discussed.

4.1. Experimental observable

The emission spectrum I of an excited singlet state can be written quite generally as a double integral over all the ground and excited states configurations, where each configuration is represented by a point of the phase space, which includes all relevant degrees of freedom of the molecule in the time window of the experiment. in the following we employ a quite general definition of the observable unregarding the particular nature of the chosen set of coordinates. We shall use the symbol $\boldsymbol{Y}_{\mathrm{o}}$ to represent a given con-

figuration of the ground state, whereas $\boldsymbol{Y}$ will be employed to describe the excited state.

For the case of experiments performed in linearly polarized light, the signal is given, neglecting constant factors depending on the instrumental apparatus, by the expression [16]:

$$I(\omega_A,\omega_E,t) = \int d\boldsymbol{Y}_{\rm o} d\boldsymbol{Y} [\boldsymbol{e}_A \cdot \boldsymbol{\mu}_A(\boldsymbol{Y}_{\rm o})]^2 g_A[\omega_A - \Delta\omega(\boldsymbol{Y}_{\rm o})] P^{(0)}(\boldsymbol{Y}_{\rm o}) \times [\boldsymbol{e}_E \cdot \boldsymbol{\mu}_E(\boldsymbol{Y})]^2 g_E[\omega_E - \Delta\omega(\boldsymbol{Y})] P(\boldsymbol{Y}_{\rm o},\boldsymbol{Y},t)\,. \quad (57)$$

Here $\boldsymbol{e}_{A,E}$ are the directions of the polarization vectors for the absorption and emission light, respectively; $\boldsymbol{\mu}_A(\boldsymbol{Y}_{\rm o})$ and $\boldsymbol{\mu}_E(\boldsymbol{Y})$ are the transition dipole moments; $\omega_{A,E}$ are the absorption and emission frequencies; $g_{A,E}$ are band-shape functions in absorption and emission, centered at the frequency $\Delta\omega(\boldsymbol{Y}_{\rm o})$ and $\Delta\omega(\boldsymbol{Y})$, respectively, related to the difference in energy between the two states for a given point $\boldsymbol{Y}$ of the phase space

$$\Delta\omega(\boldsymbol{Y}) = [E_1(\boldsymbol{Y}) - E_0(\boldsymbol{Y})]/\hbar\,. \quad (58)$$

Eq. (58) requires, to be complete, the knowledge of the Boltzmann equilibrium distribution for the ground state, $P^{(0)}(\boldsymbol{Y}_{\rm o})$ and the distribution at time t for the excited state, $P(\boldsymbol{Y}_{\rm o},\boldsymbol{Y},t)$ which depends parametrically also on $\boldsymbol{Y}_{\rm o}$ through the initial conditions. A time evolution operator $\hat{\Gamma}$ for the distribution in the excited state can be introduced. The time evolution equation is then obtained including a source term $S(\boldsymbol{Y}_{\rm o},\boldsymbol{Y},t)$ and a sink term $k_E(\boldsymbol{Y})$ [1]:

$$\frac{\partial}{\partial t} P(\boldsymbol{Y}_{\rm o},\boldsymbol{Y},t) = -[\hat{\Gamma} + k_E(\boldsymbol{Y})] P^{(1)}(\boldsymbol{Y}_{\rm o},\boldsymbol{Y},t) + S(\boldsymbol{Y}_{\rm o},\boldsymbol{Y},t) \quad (59)$$

$$P(\boldsymbol{Y}_{\rm o},\boldsymbol{Y},0) = 0\,, \quad (60)$$

which is formally solved to give:

$$P(\boldsymbol{Y}_{\rm o},\boldsymbol{Y},t) = \int_0^t d\tau \exp\{-[\hat{\Gamma} + k_E(\boldsymbol{Y})]\tau\} S(\boldsymbol{Y}_{\rm o},\boldsymbol{Y},t-\tau)\,. \quad (61)$$

In the following Sections, our main interest will lie in simulating emission spectra, so that a fixed frequency of absorption ω_A can be chosen. The sink, source and absorption band shape functions can also be simplified: *(a)* the sink function $k_E(\boldsymbol{Y})$, responsible for the decay of the population of the excited state is taken as a simple exponential decay with time constant given by the fluorescence life-time τ_F; for sake of simplicity we assume $k_E(\boldsymbol{Y})$

to be independent on the configuration coordinate $\boldsymbol{Y}$ (see ref. [17] for a discussion on the wavelength dependence of $k_E(\boldsymbol{Y})$); *(b)* the source function $S(\boldsymbol{Y}_{\rm o}, \boldsymbol{Y}, t)$ is chosen as the product of two Dirac delta functions in space and time:

$$S(\boldsymbol{Y}_{\rm o}, \boldsymbol{Y}, t) = \delta(\boldsymbol{Y}_{\rm o} - \boldsymbol{Y})\delta(t)\,, \tag{62}$$

i.e. an instantaneous, point-to-point excitation from the ground to excited state is allowed; *(c)* the dependence of the band shape function, $g_A[\omega_A - \Delta\omega(\boldsymbol{Y}_{\rm o})]$, upon $\boldsymbol{Y}_{\rm o}$, at the selected frequency of absorption ω_A, is neglected. The following simplified expression for $I(t)$ is then obtained (systematically neglecting constant factors)

$$\begin{aligned} I(\omega_E, t) \;=\; & \exp(-t/\tau_F) \int d\boldsymbol{Y} [\boldsymbol{e}_E \cdot \boldsymbol{\mu}_E(\boldsymbol{Y})]^2 g_E[\omega_E - \Delta\omega(\boldsymbol{Y})] \\ & \times \exp(-\hat{\Gamma} t)[\boldsymbol{e}_A \cdot \boldsymbol{\mu}_A(\boldsymbol{Y})]^2 P^{(0)}(\boldsymbol{Y})\,. \end{aligned} \tag{63}$$

Eq. (63) can be used to interpret the emission fluorescence signal in linearly polarized light. Notice that the time distribution function of the excited state is depending directly on the ground state equilibrium distribution and on the projection of the *absorption* transition moment upon the polarization plane of the exciting radiation.

We may now proceed to specialize our methodology to an experimental setup of interest. Let us consider a rigid emitting solute molecule (probe) which is reorienting in a polar environment. The medium may exists either in an ordered (nematic) or in an isotropic phase. The relevant set of coordinates is then chosen accordingly; first, the orientation of the probe molecule has to be included, represented by a set of Euler angles $\boldsymbol{\Omega} = \alpha, \beta, \gamma$ which define the MF orientation with respect to the laboratory frame (LF). If a cylindrical symmetry is assumed for the molecule the azimuthal angle γ is separated (see below).

4.2. Dynamics

We need to define the time evolution operator $\hat{\Gamma}$. We adopt a purely diffusive description for both coordinates, $\boldsymbol{\Omega}_{\rm o}$ and $\boldsymbol{R}$. The complete time evolution operator is then given by Eq. (33). Two diffusional tensors, $\boldsymbol{D}_R$ for the rotation, diagonal in the molecular frame, and $\boldsymbol{D}_S$ for the solvent polarization, diagonal in the laboratory frame, need to be defined. Assumptions can still be made to simplify the treatment: the simple potential given by Eq. (3) is chosen for for the orientational interaction, both in the ground and excited states, *i.e.* the assumption is made that the steric interaction in the two states are essentially the same. Next, dipole vectors $\boldsymbol{\mu}_{\rm o}$ and $\boldsymbol{\mu}_1$

are assumed to be aligned to the z-axis of the molecular frame; *i.e.* in the laboratory frame, for $i = 0, 1$:

$$\boldsymbol{\mu}_i = \mu_i \boldsymbol{z}(\boldsymbol{\Omega}_\mathrm{o}) \,, \tag{64}$$

where $\boldsymbol{z} = (\cos\alpha_\mathrm{o} \sin\beta_\mathrm{o}, \sin\alpha_\mathrm{o} \sin\beta_\mathrm{o}, \cos\beta_\mathrm{o})^\mathrm{tr}$. Since no explicit coupling with the azimuthal angle γ is present, the parallel tumbling time $\tau_R^{\parallel}$ does not enter the calculation of correlation functions for observables not depending upon γ. A further hypothesis is made when noticing that the anisotropy of both tensors $\boldsymbol{F}_\mathrm{or}$ and $\boldsymbol{F}_\infty$ is rather small, since for reasonable values of dielectric constants the difference between perpendicular and parallel components is less than 2 %. In the following we shall consider both tensors as isotropic, $\boldsymbol{F}_\mathrm{or} = F_\mathrm{or}\mathbf{1}$ and $\boldsymbol{F}_\infty = F_\infty \mathbf{1}$.

The final time-evolution operator describing the rotation of the probe in its excited state, is finally given in terms of the coordinates $\boldsymbol{Y} = \boldsymbol{\Omega}, \boldsymbol{R}$, and the potential energy is

$$V(\boldsymbol{Y}) \equiv E_1(\boldsymbol{Y}) = -\gamma \mathrm{P}_2(\cos\beta_\mathrm{o}) - \mu_1 \boldsymbol{z}(\boldsymbol{\Omega}_\mathrm{o})\boldsymbol{R} + \frac{1}{2F_\mathrm{or}}\boldsymbol{R}^2 \tag{65}$$

minus constant terms. The static properties of the systems are now defined essentially in terms of parameters which can be, at least roughly, estimated or predicted: λ can be obtained by calculations of orienting potentials; μ_0 can be evaluated by standard semi-empirical electronic calculations; μ_1 can be measured from the polarity of various solvents using the Lippert–Mataga relation; F_{or} is given in terms of dielectric parameters. The dynamical parameters are also, in principle, measurable or approximately known: $\tau_R \equiv \tau_R^{\perp}$ from the Stokes–Einstein relation and the solvent viscosity, $\tau_S^{\perp,\parallel}$ from dielectric relaxation experiments. In practice, many of these quantities are ill-defined or difficult to measure, but at least an estimate of their orders of magnitude can be given.

4.3. Correlation functions

The Stokes-shift signal is easily obtained in the form of a correlation function when the interpretation is limited to the case of completely depolarized light. An average of Eq. (63) with respect to all directions of $\boldsymbol{e}_E$ and $\boldsymbol{e}_A$ can be performed [18]. Only constant factors are generated, which can be neglected. Finally, we are left with the evaluation of the following function:

$$I(\omega, t) = \int d\boldsymbol{Y}\, g[\omega - \Delta\omega(\boldsymbol{Y})] \exp(-\hat{\Gamma} t) P^{(0)}(\boldsymbol{Y}) \,. \tag{66}$$

The straightforward dependence upon the life-time of the excited state can be neglected. The band shape function $g(\omega)$ can be estimated to be a simple Gaussian function. The intensity of the fluorescence emission at each time is centered of a frequency $\omega_{\max}(t)$ whose shift in time is defined as the Stokes shift function:

$$C(t) = \frac{\omega_{\max}(t) - \omega_{\max}(\infty)}{\omega_{\max}(0) - \omega_{\max}(\infty)} . \tag{67}$$

By neglecting any change in time of the spectral width, the frequency of maximum is identified with the averaged frequency:

$$\omega_{\max}(t) = \overline{\omega}(t) = \int d\omega \omega I(\omega, t) = \int d\boldsymbol{Y} \Delta\omega(\boldsymbol{Y}) \exp(-\hat{\Gamma} t) P^{(0)}(\boldsymbol{Y}) . \tag{68}$$

This expression can be further simplified by writing

$$P^{(0)}(\boldsymbol{Y}) = \exp[(\mu_0 - \mu_1)\boldsymbol{z}\boldsymbol{R}/k_B T] P(\boldsymbol{Y}) , \tag{69}$$

and expanding the exponential with respect to $(\mu_0 - \mu_1)/k_B T$. If the expansion is arrested to the first order term, which is acceptable if one assumes that the excited state does not differ much from the ground state dipole, after some algebra the following expression is found:

$$C(t) = \overline{(\boldsymbol{z}\boldsymbol{R} - \mu_1)(0)(\boldsymbol{z}\boldsymbol{R} - \mu_1)(t)} / \overline{(\boldsymbol{z}\boldsymbol{R} - \mu_1)^2} . \tag{70}$$

Notice that this expression depends upon a mixed function, defined with respect to $\boldsymbol{\Omega}$ and $\boldsymbol{R}$. Since $\boldsymbol{z}\boldsymbol{R} = R_3^{\mathrm{M}}$, where $\boldsymbol{R}^{\mathrm{M}}$ is the rescaled reaction field with components in the molecular frame, one can also write:

$$C(t) = \overline{R_3^{\mathrm{M}}(0) R_3^{\mathrm{M}}(t)} / \overline{R_3^{\mathrm{M}\,2}} . \tag{71}$$

The Stokes shift correlation is by definition a quantity depending upon the solvent polarization. Standard spectroscopic observables are usually given by dipolar, quadrupolar and higher ranks rotational correlation functions, which are defined for functions depending upon the probe coordinates only, analogously to the case of neutron scattering discussed in the previous Section For instance, dielectric relaxation and fluorescence depolarization are related respectively to rotational correlation functions with $j = 1$ and $j = 2$:

$$G_m^j(t) = \overline{\mathcal{D}_{m,0}^j(0) \mathcal{D}_{m,0}^j(t)} . \tag{72}$$

Notice that in both cases it is the ground state dynamics which is explored, so that the dipole moment should be defined by μ_0. In the following we shall consider a generic dipole intensity μ.

4.4. Results

The exact dependence upon time of the relevant observables can be calculated by solving numerically the dynamical problem, *i.e.* by representing the time evolution operator in matrix form in a suitable set of basis functions in $\boldsymbol{Y}$. The resulting linear algebra problem is then reduced in the usual way to the diagonalization of the matrix, to find the eigenvalues (*i.e.* the decay modes) of the problem. The correlation functions represented by Eqns. (71) and (72) are then resolved into a sum of exponentials. We represent the Smoluchowski operator in matrix form with respect to the following set of basis functions

$$\begin{aligned} |N\rangle \;\equiv\; & \left(\frac{[J_{\mathrm{o}}]}{8\pi^2}\right)^{1/2} \mathcal{D}^{J_{\mathrm{o}}}_{M_{\mathrm{o}},K_{\mathrm{o}}}(\boldsymbol{\Omega}_{\mathrm{o}})^* \\ & \times\; \mathrm{He}_{n_1}(\delta R_1/\sqrt{F_{\mathrm{or}}k_BT})\mathrm{He}_{n_2}(\delta R_2/\sqrt{F_{\mathrm{or}}k_BT})\mathrm{He}_{n_3}(\delta R_3/\sqrt{F_{\mathrm{or}}k_BT}) \\ & \times\; \exp(-\delta\boldsymbol{R}^2/4F_{\mathrm{or}}k_BT)/(2\pi)^{3/4}\,, \end{aligned} \tag{73}$$

where $\delta R_i = R_i - \mu z_i$ is the *shifted* reaction field. Matrix elements are again calculated analytically. The basis set is very similar to the one employed for the Fokker–Planck case previously analyzed; it is a standard orthonormal set. Matrices dimensions are again significantly large: truncation parameters chosen for the results presented here have been $J_{\mathrm{o}}^{\max} = 5{-}6$ and $n_i^{\max} = 5{-}6$, which correspond to dimensions between 7000 and 20000. Alternatively, calculations can be performed using a non-orthogonal basis set

$$\begin{aligned} |N\rangle \;\equiv\; & \left(\frac{[J_{\mathrm{o}}]}{8\pi^2}\right)^{1/2} \mathcal{D}^{J_{\mathrm{o}}}_{M_{\mathrm{o}},K_{\mathrm{o}}}(\boldsymbol{\Omega}_{\mathrm{o}})^* \\ & \times\mathrm{He}_{n_1}(\delta R_1/\sqrt{F_{\mathrm{or}}k_BT})\mathrm{He}_{n_2}(\delta R_2/\sqrt{F_{\mathrm{or}}k_BT}) \\ & \times\mathrm{He}_{n_3}(\delta R_3/\sqrt{F_{\mathrm{or}}k_BT})P(\boldsymbol{Y})^{1/2}\,, \end{aligned} \tag{74}$$

which is different for the presence of the weighting factor in $P(\boldsymbol{Y})$; the two basis sets are equivalent for $\gamma = 0$ (isotropic phase). For $\gamma < 3k_BT$, preliminary calculations show that the non-orthogonal basis allows to reduce the truncation factor $J_{\mathrm{o}}^{\max}$ to $3-4$. The use of non-orthogonal basis sets for the numerical solution of stochastic models is probably a very promising computational methodology for multidimensional problems. A systematic exploration of this technique is under way (see next Section).

The complete numerical approach should be followed when the time-scales of the various processes involved (rotation and solvent relaxation) are relatively close, so that clear separation of time-scales is difficult. Simplified treatments are possible when the anisotropy of diffusion $\sigma = \tau_R/\tau_S$, where τ_S is the averaged solvent correlation time, is significantly different from 1.

We employ the methodology introduced in Ref. [2] to treat asymptotically multidimensional Fokker–Planck or Smoluchowski which can be considered as the equivalent of the Born–Oppenheimer (BO) treatment of Schrödinger operators for electrons-nuclei systems. We shall consider two distinct cases. In the first case, slow probe tumbling (or fast solvent relaxation) *i.e.* $\sigma >> 1$ or $\tau_R >> \tau_S^{\perp,\parallel}$. We may then separate our coordinates in a slow set $\boldsymbol{\Omega}_o$ and in a fast set $\boldsymbol{R}$. In the case of the Stokes shift signal the approximated result is obtained in the simple form

$$C(t) = \frac{2(1-\overline{\mathrm{P}_2})}{3} e^{-t/\tau_S^{\perp}} + \frac{2\overline{\mathrm{P}_2}+1}{3} e^{-t/\tau_S^{\parallel}} . \tag{75}$$

For an isotropic system $S = 0$ and $\tau_S^{\perp} = \tau_S^{\parallel} \equiv \tau_S$:

$$C_{\mathrm{iso}}(t) = e^{-t/\tau_S} , \tag{76}$$

i.e. only the solvent relaxation times are explicitly present. Next let us consider a generic rotational correlation function, $G_m^j(t)$, defined by Eq. (72). In this case the solvent appears not the influence the observed time decay, which assumes, in the isotropic case, the analytical form:

$$G_{m\,\mathrm{iso}}^j(t) = e^{-j(j+1)t/\tau_R} , \tag{77}$$

whereas in the case of a liquid crystal phase will be obtained solving numerically the dynamical problem defined by Eq. (72) with the one-body Smoluchowski operator defined with respect to the potential V_{mf}. Thus our conclusions concerning the regime of slow tumbling, or fast solvent relaxation can be summarized as follows: standard rotational correlation functions, which depend upon the probe coordinates only, do not depend at all on the solvent relaxation. On the contrary, the Stokes-shift function has no slow decaying component, and it is completely determined by the solvent relaxation.

The dynamical regimes obtained for a fast tumbling motion and relatively slow solvent relaxation, *i.e.* $\tau_R \ll \tau_S^{\perp,\parallel}$, or $\sigma << 1$ are more complex, but of some interest since for complex solvents the dielectric relaxation times can be of the order of nanoseconds and the rotational correlation time τ_R of the solute molecule can be comparable in magnitude or even smaller. In general, however, the Stokes shift correlation function behaviour in the limit of slow solvent is relatively complex, even in the isotropic case: it contains a slow decay term, which depends upon the solvent decay times and represents the evolution of the slow relaxing polarization in the potential obtained after averaging the fast rotational coordinates; and a fast decay term, which

becomes negligible in the limit of strong coupling, which is essentially obtained by an inhomogeneous average, with respect to all possible value of the polarization vector, of rotational dipolar correlation functions. Detailed expressions are reported elsewhere [19].

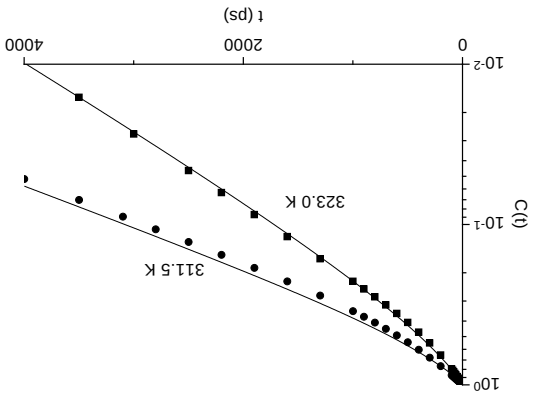

Fig. 5. Experimental (dots) and simulated (lines) Stokes shift decay curves at $T = 311.5$ K and $T = 323$ K, for coumarin C503 in ZLI 1167.

Actual experiments have been recently performed to measure time resolved fluorescence emission of coumarins in liquid crystals which meet most of the practical requirements [11]: coumarin 503 (C503) in ZLI 1167, a nematic eutectic mixture of 4-alkyl-4'-carbonitril-bicyclohexyl. C503 is a rigid molecule, which does not show photo-physical processes in the excited state; it shows a non-structured fluorescence band well separated from the absorption band. Finally, ZLI 1167 has the main advantages of being transparent in the region under investigation and of having a nematic phase at relatively low temperature. The interpretation of the available experimental results has been carrier extensively in another work [11]. Here we show some selected results. In Fig. 5 two experimental and simulated Stokes shift decay curves are shown, for $T = 311.5$ K and $T = 323$ K: the agreement between theory and experiment is rather good, and all parameters, both static and dynamics, have been estimated from existing data in the literature. The analysis of several decay curves taken at different temperatures shows that the relaxation dynamics is clearly bi-exponential in the nematic phase ($\gamma \neq 0$, $\tau_S^{\perp} < \tau_S^{\parallel}$) and it becomes nearly mono-exponential in the isotropic phase. Due to the influence of the solvent coordinates, the Stokes shift correlation function has a weaker dependence upon temperature of simple rotational correlation functions. In Fig. 6, we show a series of calculated first rank correlation function, $G_0^1(t)$, for several temperatures. The temperature dependence of the effective correlation times relative to the calculated $G_0^1(t)$ and $C(t)$ are reported in Fig. 7. The correlation times are calculated

as time integrals of the corresponding correlation functions. The first rank orientational correlation function is expected to be strongly influenced by the presence of a nematic barrier, and in fact at the isotropic-nematic transition, a relatively large increase, of *ca.* 130%, for the correlation time is obtained. The value of *ca.* 10 ns at 311.5 K, is not unreasonable compared with parallel dielectric relaxation times of other liquid crystals in the same range of temperature and viscosity.

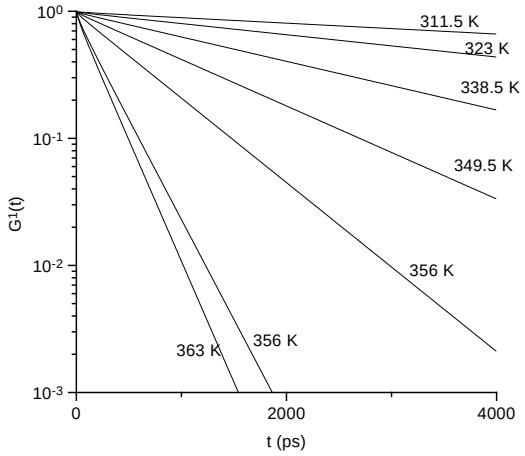

Fig. 6. Calculated first rank correlation function, $G_0^1(t)$, for several temperatures.

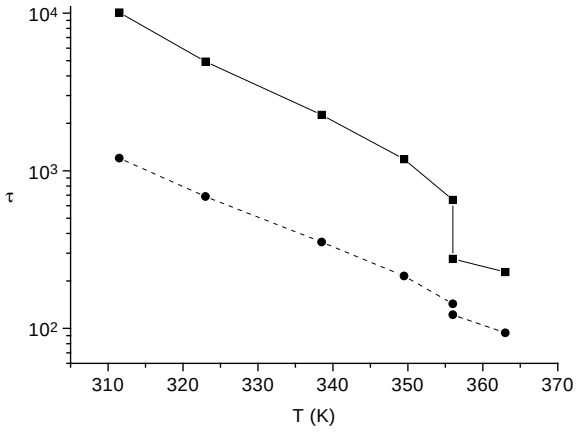

Fig. 7. Correlation times relative to the calculated $G_0^1(t)$ (full line) and $C(t)$ (dashed line).

On the contrary, the Stokes shift correlation function shows a qualitatively different behaviour. First we note that the values of correlation times at various temperatures are much lower than the corresponding values of

the orientational first rank correlation function. More interesting is the observation that the isotropic-nematic transition does not affect significantly the $C(t)$ function, as observed experimentally, the change for the correlation time at the transition temperature being of *ca.* 15%.

5. The cage model for a linear rotator

Finally we shall consider the case of an isotropic non-polar fluid and the application of an extended Fokker–Planck stochastic model to the interpretation of the rotational motion of an axially symmetric probe, coupled to a diffusional cage. The cage model for the rotational motion of a linear molecule is based on a series of hypothesis which define the static and dynamic property of the system: *(a)* a generic molecule (probe) is represented as a rotator; the translational degrees of freedom of the probe are neglected, as they are essentially uncoupled (neglecting any hydro-dynamical roto-translational coupling) from the rotations; *(b)* the local environment is made by a cluster of molecules (cage) and it behaves as a diffusive rigid body, subjected to random changes in its internal structure; *(c)* the interaction potential between probe and cage is responsible for fast confined librations of the probe: the overall motion is then given by the superposition of the rotation of the cage, the librations of the probe, and the random restructuring process of the cage potential. After defining the phase space and the time evolution law for the system, we shall proceed to consider explicitly the fast and slow processes, in order to solve the dynamics on the basis of the separation of timescales

5.1. Phase space

According to Refs [2, 4] the phase space describing axially symmetric molecule rotating in the field generated by a cage solvent structure is given by the collection of variables

$$\boldsymbol{Y} = (\boldsymbol{\Omega}_{\mathrm{o}}, \boldsymbol{L}, \boldsymbol{\Omega}_{\mathrm{c}}, \omega)\,. \tag{78}$$

It is preferred to change the representation of the time evolution operator to the following set of variables

$$\boldsymbol{X} = (\boldsymbol{\Omega}, \boldsymbol{L}, \boldsymbol{\Omega}_{\mathrm{c}}, \omega)\,, \tag{79}$$

where $\boldsymbol{\Omega} = (\alpha, \beta, \gamma)$ has been defined in Section 2 as the the relative orientation of the molecular frame with respect to the cage frame.

The system potential energy is written by including only the leading terms with respect to the ranks of Wigner functions in $\boldsymbol{\Omega}$ in the following

form:

$$V(\boldsymbol{\Omega},\omega) \equiv V_{\rm c}(\boldsymbol{\Omega},\omega) = -I_{\perp}\omega^2 \mathcal{D}^2_{0,0}(\boldsymbol{\Omega})/3\,. \tag{80}$$

The time evolution operator is now specified according to the idea that the system $\boldsymbol{X}$ constitutes a closed Markovian space whose temporal evolution is dictated by single elementary processes represented by Fokker–Planck or diffusive terms. The non-equilibrium distribution is obtained from the solution of the general equation:

$$\partial P(\boldsymbol{X},t)/\partial t = -\hat{\Gamma} P(\boldsymbol{X},t)\,. \tag{81}$$

The operator $\hat{\Gamma}$ is obtained as the sum of three terms

$$\hat{\Gamma} = \hat{\Gamma}_{\rm solute} + \hat{\Gamma}_{\rm cage\ rot.} + \hat{\Gamma}_{\rm cage\ rest.}\,, \tag{82}$$

which have been defined in Section 2 with respect to coordinates $\boldsymbol{Y}$: they describe the solute Fokker–Planck dynamics, the rotational diffusion of the cage and the restructuring of the cage, respectively. The solute term can be written in $\boldsymbol{X}$ just by substituting $\hat{\boldsymbol{M}}(\boldsymbol{\Omega}_{\rm o})$ with $\hat{\boldsymbol{M}}(\boldsymbol{\Omega})$ [2].

The rotational diffusion motion of cage is described, in the $\boldsymbol{X}$ phase space according to the expression

$$\begin{aligned}\hat{\Gamma}_{\rm cage\ rot.} \;=\; & -D[\hat{\boldsymbol{M}}(\boldsymbol{\Omega}_{\rm c}) - \boldsymbol{E}(\boldsymbol{\Omega})\hat{\boldsymbol{M}}(\boldsymbol{\Omega})]^{\rm tr} P(\boldsymbol{X}) \\ & \times[\hat{\boldsymbol{M}}(\boldsymbol{\Omega}_{\rm c}) - \boldsymbol{E}(\boldsymbol{\Omega})\hat{\boldsymbol{M}}(\boldsymbol{\Omega})] P(\boldsymbol{X})^{-1}\,.\end{aligned} \tag{83}$$

The third term, for the random restructuring of the cage, has again the form of a master equation which describes the interchange between two given configuration $\boldsymbol{X}$ and $\boldsymbol{X}'$:

$$\hat{\Gamma}_{\rm cage\ rest.}\, P(\boldsymbol{X},t) = \int d\boldsymbol{X}'[P(\boldsymbol{X},t)W(\boldsymbol{X}\to\boldsymbol{X}') - P(\boldsymbol{X}',t)W(\boldsymbol{X}'\to\boldsymbol{X})]\,, \tag{84}$$

with a transition kernel $W(\boldsymbol{X}\to\boldsymbol{X}')$ dependent in general on the initial configuration $\boldsymbol{X}$ and the final one $\boldsymbol{X}'$, which is now written as:

$$W(\boldsymbol{X}\to\boldsymbol{X}') = \mathcal{W}(\boldsymbol{\Omega}_{\rm c} - \boldsymbol{\Omega}'_{\rm c})\delta(\boldsymbol{\Omega}' + \boldsymbol{\Omega}'_{\rm c} - \boldsymbol{\Omega}_{\rm c} - \boldsymbol{\Omega})\delta(\boldsymbol{L}' - \boldsymbol{L})P(\boldsymbol{\Omega}',\omega') \tag{85}$$

according to Eq. (21).

5.2. Fast and slow processes

Our purpose is to evaluate the auto-correlation function for the generic observable $f(\boldsymbol{X})$

$$G(t) = \overline{f[\boldsymbol{X}(0)]f[\boldsymbol{X}(t)]} = \int d\boldsymbol{X}\, f(\boldsymbol{X})^* \exp(-\hat{\Gamma}t) f(\boldsymbol{X}) P(\boldsymbol{X})\,. \tag{86}$$

We shall specifically analyze the correlation functions probing the solute dynamics and which are required in the interpretation of spectroscopic observations [20]. For the solute orientation we shall consider the spherical harmonics which can be specified as Wigner functions of the first two angles of $\boldsymbol{\Omega}_{\rm o} = (\alpha_{\rm o}, \beta_{\rm o}, \gamma_{\rm o})$, *i.e.* correlation function $G^j_m(t)$: index m can be neglected due to the absence of mean field potential, *i.e.* due the isotropy with respect to the laboratory frame. It is also of relevance the correlation function for the component of the angular momentum perpendicular to the long axis of the molecular frame, defined as

$$G^L(t) \equiv \overline{\boldsymbol{L}_\perp(0) \cdot \boldsymbol{L}_\perp(t)}\,. \tag{87}$$

It should be evident that exact solutions for the correlation functions are derivable only numerically. In Ref. [4], a full numerical solution of a closely related problem, in which the solute dynamics is described by a linear rotator instead of a axially symmetric rigid body, has been worked out, and examples have been shown of correlation functions and spectroscopical observables related to them which have been obtained through *(i)* the matrix representation of the time evolution operator on a complete set of basis functions and *(ii)* the direct diagonalization of the resulting matrix. The procedure was shown to be very effective, although the number of coupled degrees of freedom to be considered is relatively high. However, a full exploration of the entire range of parameters and dynamical regimes predicted by the model can be also accomplished by some totally or partially analytical approximated treatment. Full numerical solution can then be used for 'fine tuning' of the model, to better relate simulation results with experimental measurements.

To summarize, the cage model is fully specified once a value is attributed to the parameters $\omega_s = \sqrt{k_B T/I}$ (streaming frequency), $\tau_{\rm c} = I_\perp/\xi_\perp$ (collisional time), D (cage diffusion coefficient), and functional forms have been defined for $P(\omega)$ and $\mathcal{W}(\boldsymbol{\Omega}_{\rm c} - \boldsymbol{\Omega}'_{\rm c})$. Notice that dependence upon $I_\parallel$ and $\xi_\parallel$ is absent due to the axial symmetry of the cage potential, *i.e.* $\gamma_{\rm c}$, γ and $L^{\rm M}_z$ are uncoupled coordinates. For later use we introduce the equilibrium distribution on the cage variables only

$$P_S(\boldsymbol{X}_S) \equiv \int d\boldsymbol{X}_F P(\boldsymbol{X}_F, \boldsymbol{X}_S) = P(\omega)/8\pi^2 \tag{88}$$

is independent of the cage orientation $\boldsymbol{\Omega}_{\rm c}$. Correspondingly the full equilibrium distribution is conveniently factorized as

$$P(\boldsymbol{X}_F, \boldsymbol{X}_S) = P_S(\boldsymbol{X}_S) P(\boldsymbol{X}_S | \boldsymbol{X}_F)\,, \tag{89}$$

where $P(\boldsymbol{X}_S|\boldsymbol{X}_F) = P(\omega|\boldsymbol{\Omega}, \boldsymbol{L})$ is the conditional probability of fast variables for a given set $\boldsymbol{X}_S$ of slow variables. which is also independent of the

cage orientation $\boldsymbol{\Omega}_c$. Such a distribution should be sharply peaked about the solute stationary state at $\beta = 0$, in order to be consistent with the derivation of the cage potential as an expansion about the potential minimum.

5.3. Slow cage dynamics

By taking for granted the time scale separation between fast librational motions and slow cage dynamics, we examine in this section the relaxation of the slow variables $\boldsymbol{X}_S = (\boldsymbol{\Omega}_c, \omega)$. The general techniques for treating stochastic problems characterized by variables with different time scales has been discussed in Ref. [2] (see in particular its Appendix B) on the basis of the analogy with the Born–Oppenheimer method of quantum mechanics. Here we shall apply that method to the axial cage model presented in the previous section.

The behavior of the system at long time scales is determined by the relaxation of the slow variables only, and it is described by a distribution contracted on the fast variables $\boldsymbol{X}_F$

$$P_S(\boldsymbol{X}_S, t) \equiv \int d\boldsymbol{X}_F P(\boldsymbol{X}_F, \boldsymbol{X}_S, t)\,. \tag{90}$$

The projection onto the subspace of functions of slow variables supplies the required time evolution equation

$$\partial P_S(\boldsymbol{X}_S, t)/\partial t = -\hat{\Gamma}_S P_S(\boldsymbol{X}_S, t)\,, \tag{91}$$

with the projected operator $\hat{\Gamma}_S$ defined implicitly by the identity

$$\hat{\Gamma}_S g(\boldsymbol{X}_S) P_S(\boldsymbol{X}_S) \equiv \int d\boldsymbol{X}_F \hat{\Gamma} P(\boldsymbol{X}) g(\boldsymbol{X}_S) \tag{92}$$

for any $g(\boldsymbol{X}_S)$. A slow component is extracted from any function $f(\boldsymbol{X})$ in the following form

$$f_S(\boldsymbol{X}_S) \equiv \int d\boldsymbol{X}_F f(\boldsymbol{X}) P(\boldsymbol{X}_S | \boldsymbol{X}_F)\,. \tag{93}$$

Correspondingly in the autocorrelation function $G(t)$ of Eq. (86), a slow component $G_S(t)$ is identified by the relation [2]

$$G_S(t) = \int d\boldsymbol{X}_S f_S(\boldsymbol{X}_S)^* \exp(-\hat{\Gamma}_S t) f_S(\boldsymbol{X}_S) P_S(\boldsymbol{X}_S)\,. \tag{94}$$

By inserting into Eq. (91) the evolution operator defined in the previous section, the following equation is obtained

$$\frac{\partial}{\partial t}P_S(\boldsymbol{X}_S,t) \equiv \hat{\boldsymbol{M}}(\boldsymbol{\Omega}_\mathrm{c})^\mathrm{tr}\boldsymbol{D}\hat{\boldsymbol{M}}(\boldsymbol{\Omega}_\mathrm{c})P_S(\boldsymbol{X}_S,t)$$
$$+\int d\boldsymbol{X}'_S[P_S(\boldsymbol{X}'_S,t)W_S(\boldsymbol{X}'_S\rightarrow\boldsymbol{X}_S)-P_S(\boldsymbol{X}_S,t)W_S(\boldsymbol{X}_S\rightarrow\boldsymbol{X}'_S)] \tag{95}$$

without contributions from $\hat{\Gamma}_\mathrm{solute}$ since it operates on fast variables only. The first term at the r.h.s. of Eq. (95) derives from the cage rotation operator (83) after elimination of the rotation operator $\hat{\boldsymbol{M}}(\boldsymbol{\Omega})$ on the relative orientation $\boldsymbol{\Omega}$ belonging to the set of fast variables. The other term is the result of the projection of the Master Equation (20) for the cage restructuring, with the following reduced kernel W_S for transitions of slow variables

$$W_S(\boldsymbol{X}_S\rightarrow\boldsymbol{X}'_S)\equiv 8\pi^2\mathcal{W}(\Delta\boldsymbol{\Omega}_\mathrm{c})P_S(\boldsymbol{X}'_S)\int d\boldsymbol{\Omega}P_\omega(\boldsymbol{\Omega})P_{\omega'}(\boldsymbol{\Omega}-\Delta\boldsymbol{\Omega}_\mathrm{c})\,, \tag{96}$$

where $P_\omega(\boldsymbol{\Omega})$ is the Boltzmann distribution with respect to $V_\mathrm{c}(\boldsymbol{\Omega},\omega)$, normalized in $\boldsymbol{\Omega}$:

$$P_\omega(\boldsymbol{\Omega})=\exp[-V_\mathrm{c}(\boldsymbol{\Omega},\omega)/k_BT]\Big/\int d\boldsymbol{\Omega}\exp[-V_\mathrm{c}(\boldsymbol{\Omega},\omega)/k_BT]\,. \tag{97}$$

If one assumes

$$\mathcal{W}(\Delta\boldsymbol{\Omega}_\mathrm{c})\equiv\mathcal{W}(|\Delta\beta_\mathrm{c}|)\,, \tag{98}$$

then it is possible to show that $W_S(\boldsymbol{X}_S\rightarrow\boldsymbol{X}'_S)/P_S(\boldsymbol{X}'_S)$, *i.e.* the reduced kernel for a transition $\boldsymbol{X}_S\rightarrow\boldsymbol{X}'_S$, is a symmetric function in $|\Delta\beta_\mathrm{c}|$.

The simple structure of the evolution operator $\hat{\Gamma}_S$ for the slow variables, allows the analytical derivation of the slow decaying part of the orientational correlation function. No slow component is recovered for the correlation function Eq. (87) of the angular momentum, since the corresponding projected functions f_S vanish. On the contrary a large contribution of the cage dynamics is found for the solute rotational motion. The orientational observable is conveniently written as

$$f=\mathcal{D}^j_{m,0}(\boldsymbol{\Omega}_\mathrm{o})=\sum_k\mathcal{D}^j_{m,k}(\boldsymbol{\Omega}_\mathrm{c})\mathcal{D}^j_{k,0}(\boldsymbol{\Omega}) \tag{99}$$

from which the following slow component is derived

$$f_S=\mathcal{D}^j_{m,0}(\boldsymbol{\Omega}_\mathrm{c})d^j(\omega)\,, \tag{100}$$

with coefficients

$$d^j(\omega) \equiv \int d\boldsymbol{\Omega} \mathcal{D}^j_{0,0}(\boldsymbol{\Omega}) P_\omega(\boldsymbol{\Omega}) \,. \tag{101}$$

One can expand the generic solution of Eq. (95) in terms of Wigner functions of $\boldsymbol{\Omega}_\mathrm{c}$, $\mathcal{D}^j_{m,k}(\boldsymbol{\Omega}_\mathrm{c})$ and then solve for the unknown expansion coefficients in ω and t, which are obtained from a master equation in ω only. In particular, under condition (98), the only relevant function for the correlation function corresponding to Eq. (100) is given by

$$\begin{aligned} \frac{\partial}{\partial t} P_j(\omega, t) \; &= \; -D_\perp j(j+1) P_j(\omega, t) \\ &\quad + \int d\omega' [P_j(\omega', t) w(\omega' \to \omega) - P_j(\omega, t) w(\omega \to \omega')] \,, \end{aligned} \tag{102}$$

where the initial condition is

$$P_j(\omega, 0) = d^j(\omega) P(\omega) \,, \tag{103}$$

and the reduced kernel is:

$$w(\omega \to \omega') = \int d\boldsymbol{\Omega}_\mathrm{c} d\boldsymbol{\Omega}'_\mathrm{c} W_S(\boldsymbol{X}_S \to \boldsymbol{X}'_S) \,. \tag{104}$$

It follows that the slow part of the correlation function for the probe rotation is given by the following expression

$$G^j_S(t) = \frac{1}{2j+1} \exp[-j(j+1) D_\perp t] \int d\omega P_j(\omega, 0) P_j(\omega, t) \,, \tag{105}$$

which is independent from the parallel component $D_\parallel$ of the diffusion tensor. Expression (105) shows that the slow decaying component of the probe rotational correlation function has a Brownian-like dependence upon rank [constant $j(j+1)$ term] and a correction factor due to cage restructuring, which is intrinsically multi-exponential.

5.4. Fast librational motions.

In the hypothesis that a well defined separation exists between the time scales of cage dynamics and of solute librational motions, the evolution of fast variables $\boldsymbol{X}_F = (\boldsymbol{\Omega}, L)$ can be analyzed separately [2]. First one isolates from the full evolution operator $\hat{\Gamma}$ the part $\hat{\Gamma}_F$ which operates on the fast variables only. In the following calculations we assume that

$$\hat{\Gamma}_F = \hat{\Gamma}_\mathrm{solute} \tag{106}$$

by neglecting the contributions of the cage terms, for instance the terms of $\hat{\Gamma}_{\text{cage rot.}}$ Eq. (83) with rotation operators acting on $\boldsymbol{\Omega}$. The same separation of the two types of motions justifies such an approximation as long as it requires the condition $|\hat{\Gamma}_{\text{solute}}| >> |\hat{\Gamma}_{\text{cage rot.}} + \hat{\Gamma}_{\text{cage rest.}}|$ for their typical rates. However, it breaks down when the friction ξ vanishes, and a purely conservative dynamics is described by $\hat{\Gamma}_{\text{solute}}$ without any relaxation to equilibrium. Then the cage terms become the main source of relaxation also of the probe coordinates, and their contribution cannot be neglected in $\hat{\Gamma}_F$. Approximation Eq. (54) is legitimate when the relaxation of fast variables is driven mainly by the frictional operator, that is if

$$1/\tau_{\text{c}} >> D_{\perp}, w \tag{107}$$

$1/\tau_{\text{c}}$ being the typical rate for the collisional part of $\hat{\Gamma}_{\text{solute}}$, with the contributions of cage rotations and cage restructuring estimated according to their rate coefficients.

Hereafter we shall taken for granted the condition Eq. (107), by calculating non-equilibrium distributions on the fast variables according to Eq. (54). It should be emphasized that $\hat{\Gamma}_F$ which operates on $\boldsymbol{X}_F$ variables, has also a parametric dependence on the slow variables, in particular on the librational frequency ω which determines the strength of the cage potential. Therefore its solutions are parametrically dependent on the slow variables $\boldsymbol{X}_S$, and in the conditional probability of $\boldsymbol{X}_F$ at time t with initial condition $\boldsymbol{X}_F^0$ at time $t = 0$ one should specify also the value of $\boldsymbol{X}_S$:

$$P(\boldsymbol{X}_S, \boldsymbol{X}_F^0 | \boldsymbol{X}_F, t) = \exp(-\hat{\Gamma}_F t)\delta(\boldsymbol{X}_F - \boldsymbol{X}_F^0)\,. \tag{108}$$

At asymptotically long times such a probability attains the equilibrium distribution on $\boldsymbol{X}_F$ conditioned by $\boldsymbol{X}_S$

$$\lim_{t\to\infty} P(\boldsymbol{X}_S, \boldsymbol{X}_F^0 | \boldsymbol{X}_F, t) = P(\boldsymbol{X}_S | \boldsymbol{X}_F)\,. \tag{109}$$

The separation of fast and slow processes is performed by employing the following approximation for the conditional probability on all the variables

$$\begin{aligned} P(\boldsymbol{X}^0 | \boldsymbol{X}, t) \;=\; & \delta(\boldsymbol{X}_S - \boldsymbol{X}_S^0)[P(\boldsymbol{X}_S, \boldsymbol{X}_F^0 | \boldsymbol{X}_F, t) \\ & - P(\boldsymbol{X}_S | \boldsymbol{X}_F)] + P(\boldsymbol{X}_S | \boldsymbol{X}_F) P_S(\boldsymbol{X}_S^0 | \boldsymbol{X}_S, t)\,, \end{aligned} \tag{110}$$

where $P_S(\boldsymbol{X}_S^0 | \boldsymbol{X}_S, t)$ is the conditional probability for the slow variables only to be derived as a solution of Eq. (91). The first term at the r.h.s. of Eq. (110) describes the relaxation of fast variables when the slow ones are still frozen in correspondence of their initial value $\boldsymbol{X}_S^0$. Let us consider a

time t^* which represent a time scale intermediate between those of the fast and the slow motions. At such a time Eq. (110) is simplified as

$$P(\boldsymbol{X}^0|\boldsymbol{X},t^*) \simeq \delta(\boldsymbol{X}_S - \boldsymbol{X}_S^0)P(\boldsymbol{X}_S|\boldsymbol{X}_F) \tag{111}$$

that is the slow variables have still their initial values, while the conditioned equilibrium distribution is recovered for the fast variables. At later times the relaxation of slow variables becomes operative according to the second term at the r.h.s. of Eq. (110). Within this longer time scale the fast variables are always characterized by an equilibrium distribution $P(\boldsymbol{X}_S|\boldsymbol{X}_F)$ conditioned by the value of $\boldsymbol{X}_S$. It should be emphasized that, besides the previous phenomenological justification, a formal derivation of Eq. (110) is possible by applying the Born–Oppenheimer approximation to stochastic problems, as shown in Appendix B of Ref. [2].

By calculating a generic auto-correlation function according to Eq. (110), two different contributions are identified

$$G(t) = G_S(t) + G_F(t)\,, \tag{112}$$

where $G_S(t)$ is the slow component given by Eq. (94). The time dependence of the fast part $G_F(t)$ is determined by operator $\hat{\Gamma}_F$ of Eq. (54) for the fast variables only according to the equation

$$G_F(t) = \int d\boldsymbol{X}_S P_S(\boldsymbol{X}_S) \int d\boldsymbol{X}_F \delta f(\boldsymbol{X})^* \exp(-\hat{\Gamma}_F t)\delta f(\boldsymbol{X}) P(\boldsymbol{X}_S|\boldsymbol{X}_F)\,, \tag{113}$$

where $\delta f(\boldsymbol{X})$ is the observable devoid of its slow component $f_S(\boldsymbol{X}_S)$

$$\delta f(\boldsymbol{X}) \equiv f(\boldsymbol{X}) - f_S(\boldsymbol{X}_S)\,. \tag{114}$$

Notice that because of Eq. (109), $G_F(t)$ vanishes outside the time window for the relaxation of fast variables. By taking into account the parametric dependence of $\hat{\Gamma}_F$ on the slow variables, Eq. (113) can be written as an average of $\boldsymbol{X}_S$-dependent elementary correlation functions defined in the $\boldsymbol{X}_F$ functional space. In the case of of solute orientational observables

$$\delta f = \sum_k \mathcal{D}^j_{l,k}(\boldsymbol{\Omega}_{\rm c})\delta\mathcal{D}^j_{k,0}(\boldsymbol{\Omega})\,, \tag{115}$$

where the ω-dependence has been left implicit in functions

$$\delta\mathcal{D}^j_{k,0}(\boldsymbol{\Omega}) \equiv \mathcal{D}^j_{k,0}(\boldsymbol{\Omega}) - d^j(\omega)\delta_{k,0} \tag{116}$$

one derives a fast component of the correlation function in the following form

$$\begin{aligned} G^j_F(t) \;=\; & (2j+1)\int d\omega P(\omega) \sum_l \int d\boldsymbol{\Omega} d\boldsymbol{L}\; \delta\mathcal{D}^j_{l,0}(\boldsymbol{\Omega})^* \\ & \times \exp(-\hat{\Gamma}_F t)\; \delta\mathcal{D}^j_{l,0}(\boldsymbol{\Omega}) P(\omega|\boldsymbol{\Omega},\boldsymbol{L})\,, \end{aligned} \tag{117}$$

where the integration on the cage orientation has been performed analytically. In a similar way an explicit form is derived for the correlation function of the angular momentum without a slow component. Because of the torques deriving from the cage potential, no analytical solution for the fast component of the correlation functions is available. Exact solutions can be obtained only numerically [4].

5.5. Spectroscopical observables and cage model

From the knowledge of orientational correlation functions one can calculate spectroscopic observables, like the far infrared signal of a rotating molecule and, within some approximation, the optical Kerr effect. The dielectric constant $\varepsilon = \varepsilon(\omega)$ is related to the normalised first rank correlation function of the rotating probe:

$$\frac{\varepsilon_0(\varepsilon - \varepsilon_\infty)(2\varepsilon + \varepsilon_\infty)}{\varepsilon(\varepsilon_0 - \varepsilon_\infty)(2\varepsilon_0 + \varepsilon_\infty)} = 1 - i\omega \int_0^\infty e^{-i\omega t} G^1(t)/G^1(0)\,, \tag{118}$$

where $\varepsilon_0 = \varepsilon(0)$, $\varepsilon_\infty = \varepsilon(\infty)$. The absorption coefficient $\alpha(\omega)$, *i.e.* the Poley signal or far infrared spectrum, is the obtained as the imaginary part of the wave vector $k(\omega) = \omega\sqrt{\varepsilon(\omega)}/c$ (where c is the speed of light):

$$\alpha(\omega) = \frac{\omega}{c}\sqrt{\frac{-\varepsilon'(\omega) + |\varepsilon(\omega)|}{2}}\,. \tag{119}$$

A model calculation is shown in Fig. 8, for $\varepsilon_0 = 10$ and $\varepsilon_\infty = 1$ (not unreasonable for a molecule like, *e.g.*, benzonitrile). Other parameters are

$$\omega_s = 2\mathrm{ps}^{-1} \quad \tau_\mathrm{c} = 8\mathrm{ps} \quad D_\perp = 0.2\mathrm{ps}^{-1}\,. \tag{120}$$

By comparing the simulation with actual far infrared spectrum, one can notice a substantial agreement of all qualitative features, namely the broad line shape of the band, which cannot be obtained with simpler diffusional Brownian models. Fig. 9 shows the corresponding simulated dielectric relaxation spectra.

An analysis of the model to recover the optical Kerr effect signal (OKE), even at a simplified level, is more difficult. First one assumes *i)* that only liner polarisable molecules are examined (*e.g.* CS_2), for which $\boldsymbol{\mu}(\boldsymbol{\Omega}_\mathrm{o}) = \boldsymbol{\alpha}(\boldsymbol{\Omega}_\mathrm{o})\boldsymbol{E}(t)$ and $\boldsymbol{\alpha}(\boldsymbol{\Omega}_\mathrm{o})$ is the molecular polarisability tensor, with $\alpha_\perp$ and $\alpha_\parallel$ as principal values; $\boldsymbol{E}(t)$ is the time-dependent electric field. Next *ii)* one assumes that the cage model holds in the presence of the external electric field, and that the librational frequency distribution is the same. One can

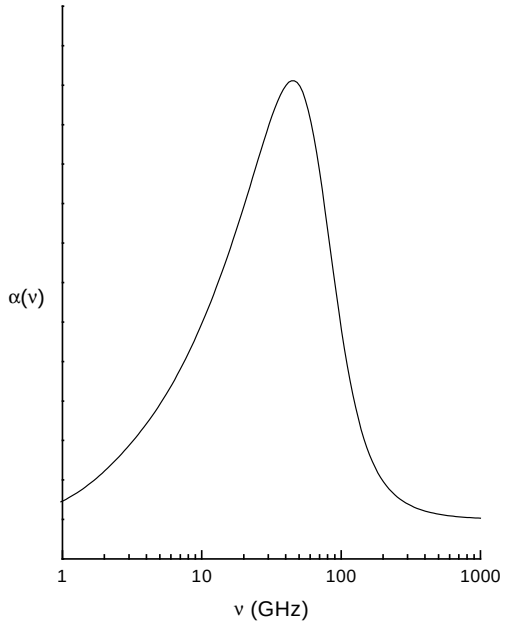

Fig. 8. Far infrared absorption signal.

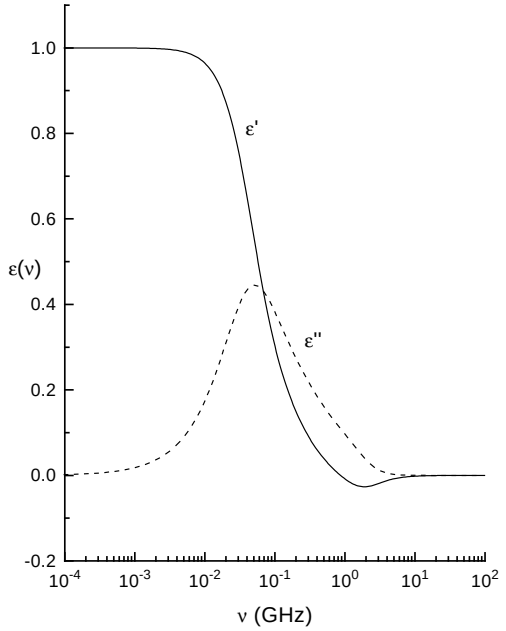

Fig. 9. Real and imaginary part of the dielectric permittivity.

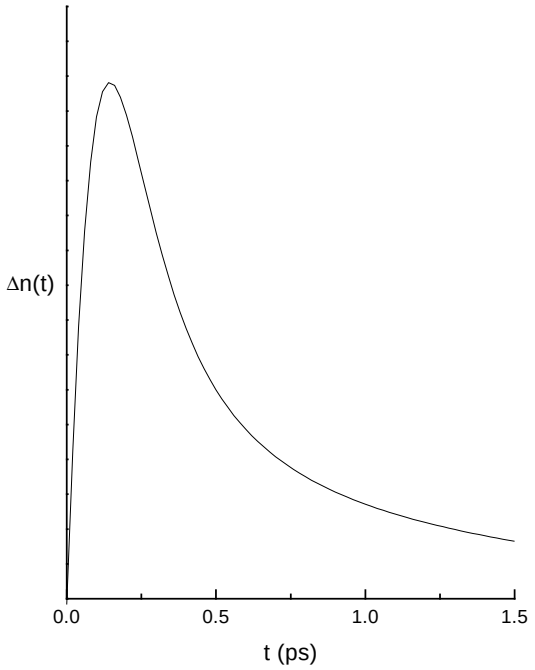

Fig. 10. Optical Kerr effect signal.

show that the cage operator previously defined is unmodified, so that the time-dependent electric field enters only in the streaming part of the solute operator. The time evolution of the distribution is then:

$$\frac{\partial}{\partial t}P(\boldsymbol{Y},t) = -[\hat{\Gamma}_0 + \hat{\Gamma}_1(t)]P(\boldsymbol{Y},t)\,, \tag{121}$$

where $\hat{\Gamma}_0$ is the time-evolution operator at $\boldsymbol{E} = 0$ and $\hat{\Gamma}_1(t)$ is the time-dependent Liouvillean defined with respect the electrostatic potential $V^{\mathrm{el}} = \boldsymbol{E}^{\mathrm{tr}}\boldsymbol{\alpha}\boldsymbol{E}$. The excitation of a typical OKE experiment can be reproduced by assuming *iii)* that

$$E_i(t)E_j(t) = \delta_{i,z}\delta_{j,z}E_{\mathrm{el}}^2\delta(t)\,. \tag{122}$$

By applying a first order perturbation treatment, whose details will be given elsewhere, one shows that birifrangence $\Delta n(t) = n_{\parallel}(t) - n_{\perp}(t) = \sqrt{\varepsilon_{\parallel}(t)} - \sqrt{\varepsilon_{\perp}(t)}$, which can be related to the OKE signal, is obtainable in terms of a simple correlation function:

$$\Delta n(t) \;=\; \frac{2\pi}{3}\frac{\mathcal{N}\Delta\alpha^2 E_{\mathrm{el}}^2}{Ik_BT\sqrt{1+4\pi\mathcal{N}\alpha_{\mathrm{iso}}}}$$

$$\times \int d\boldsymbol{Y} \mathcal{D}^2_{0,0}(\boldsymbol{\Omega}_{\rm o}) e^{-\hat{\Gamma}_0 t} P(\boldsymbol{Y})(\boldsymbol{Y}) L\hat{M}_y(\boldsymbol{\Omega}_{\rm o}) \mathcal{D}^2_{0,0}(\boldsymbol{\Omega}_{\rm o}) \,, \tag{123}$$

where $\mathcal{N}$ is the number of molecule for unit of volume, $\alpha_{\rm iso} = (2\alpha_\perp + \alpha_\parallel)/3$, $\Delta\alpha = \alpha_\parallel - \alpha_\perp$. An example of simulated OKE is shown in Fig. 10.

This work has been supported by the E.C. Human Capital and Mobility Contract: ERBCHRXCT930282 and PECO extension Contract ERB-CIPDCT940602, and in part by the Italian Ministry for Universities and Scientific and Technological Research.

Appendix A

Derivation of the $\boldsymbol{F}$ tensor

For a generic ellipsoidal body (and cavity) of volume V, the $\boldsymbol{F}$ tensor is written (in SI units):

$$\boldsymbol{F} = \frac{1}{4\pi\varepsilon_0 V} \boldsymbol{\varepsilon}^{1/2} [\boldsymbol{\varepsilon} - \boldsymbol{n}'(\boldsymbol{\varepsilon} - \boldsymbol{1})]^{-1} [(\boldsymbol{1} - \boldsymbol{n}')\boldsymbol{\varepsilon}\boldsymbol{n}'' - \boldsymbol{n}'(\boldsymbol{1} - \boldsymbol{n}'')] \boldsymbol{\varepsilon}^{-1/2} \,, \tag{124}$$

where $\boldsymbol{n}$ is the electrostatic depolarization tensor for an ellipsoidal empty cavity surrounded by the dielectric; $\boldsymbol{n}'$ is the electrostatic depolarization tensor for an ellipsoidal cavity filled by the dielectric, in vacuo; $\boldsymbol{n}''$ is simply $\boldsymbol{\varepsilon}^{-1/2}\boldsymbol{n}\boldsymbol{\varepsilon}^{1/2}$.

Operatively, $\boldsymbol{\varepsilon}$ is diagonal by definition in the LF, with principal values ε_i $(i = 1, 2, 3)$. The depolarization tensor for the cavity, is defined with respect to the auxiliary tensor $\boldsymbol{M}$ for the ellipsoid; in the LF $\boldsymbol{M}^{(L)} = \boldsymbol{E}\boldsymbol{a}^{-2}\boldsymbol{E}^{\rm tr}$, and $\boldsymbol{a}$ is the diagonal tensor whose principal values are the semi-axes of the cavity, while $\boldsymbol{E}$ is the Euler matrix which transforms a vector from the MF to the LF.

The representations of $\boldsymbol{n}$ in the LF and MF are analogously related, $\boldsymbol{n}^{(L)} = \boldsymbol{E}\boldsymbol{n}^{(M)}\boldsymbol{E}^{\rm tr}$, where the principal values $\boldsymbol{n}^{(M)}$ are given in terms of $\boldsymbol{a}$. Similarly, $\boldsymbol{n}'$ is defined in terms of an auxiliary tensor $\boldsymbol{M}'$, which in the LF is $\boldsymbol{M}'^{(L)} = \boldsymbol{\varepsilon}^{1/2}\boldsymbol{M}^{(L)}\boldsymbol{\varepsilon}^{1/2}$. For the case of a spherical cavity, $\boldsymbol{a} = a\boldsymbol{1}$, $\boldsymbol{n}^{(L)} = \boldsymbol{n}^{(M)} = \boldsymbol{1}/3$, $\boldsymbol{M}'^{(L)} = \boldsymbol{\varepsilon}/a^2$. Thus $\boldsymbol{n}'$ is diagonal in the LF, too, with components:

$$n'_i = \frac{\varepsilon_i}{2} \int_0^\infty dz \frac{1}{(1 + \varepsilon_i z)[(1 + \varepsilon_1 z)(1 + \varepsilon_2 z)(1 + \varepsilon_3 z)]^{1/2}} \tag{125}$$

and $\boldsymbol{F}$ is also diagonal in the LF, with components:

$$F_i = \frac{1}{4\pi a^3 \varepsilon_0} \frac{(1-n_i')\varepsilon_i - 2n_i'}{\varepsilon_i - n_i'(\varepsilon_i - 1)} \,. \tag{126}$$

By choosing $\varepsilon_1 = \varepsilon_2 = \varepsilon_\perp$ and $\varepsilon_3 = \varepsilon_\parallel$ the formulas reported in the main text are obtained.

REFERENCES

[1] A. Polimeno, A. Barbon, P. L. Nordio, W. Rettig, *J. Phys. Chem.* **98**, 12158 (1994); D. Braun, P. L. Nordio, A. Polimeno, G. Saielli, *Chem. Phys.* **208**, 127 (1996).

[2] A. Polimeno, G.J. Moro, J.H. Freed, *J. Chem. Phys.* **104**, 1090 (1996).

[3] P.L. Nordio, A. Polimeno, *Mol. Phys.* **75**, 1203 (1992); A. Polimeno, P.L. Nordio, *Chem. Phys. Lett.* **192**, 509 (1992).

[4] G.J. Moro, A. Polimeno, *J. Chem. Phys.* **107**, 7884 (1997).

[5] U. Segre, *Mol. Cryst. Liq. Cryst.* **90**, 239 (1982).

[6] A. Chelkowski, *Dielectric Physics*, Elsevier Scientific Company, Amsterdam 1980.

[7] P.L. Bhatnagar, E.P. Gross, M. Krook, *Phys. Rev.* **94**, 511 (1954).

[8] V.S.S. Sastry, A. Polimeno, R.H. Crepeau, J.H. Freed, *J. Chem. Phys.* **105**, 5753 (1996); **105**, 5773 (1996).

[9] K.A. Earle, J.K. Moscicki, A. Polimeno, J.H. Freed, *J. Chem. Phys.* **106**, 9996 (1997).

[10] L. Feltre, A. Polimeno, G. Saielli, P.L. Nordio, *Mol. Cryst. Liq. Cryst.* **290**, 163 (1996).

[11] G. Saielli, A. Polimeno, P.L. Nordio, P. Bartolini, M. Ricci and R. Righini, *J. Chem. Soc. Far. Trans.* **94**, 121 (1998).

[12] L. Van Hove, *Phys. Rev.* 249 (1954).

[13] A.J. Leadbetter, R.M. Richardson, in: *The Molecular Physics of Liquid Crystals*, eds. G.W. Gray and G.R. Luckhurst, London 1979, Chapp. 18 and 20.

[14] A. Belushkin, M.J. Cook, D. Frezzato, S.D. Haslam, A. Ferrarini, D. Martin, J. McMurdo, P.L. Nordio, R.M. Richardson, A. Stafford, *Mol. Phys.*, in press.

[15] A. Polimeno, J.H. Freed, *Adv. Chem. Phys.* **83**, 89 (1993).

[16] T. J. Kang, W. Jarzeba, P. F. Barbara, T. Fonseca, *Chem. Phys.* **149**, 81 (1990).

[17] M. Maroncelli, R. S. Fee, C. F. Chapman, G. R. Fleming, *J. Phys. Chem.* **95**, 1012 (1991).

[18] A. Arcioni, F. Bertinelli, R. Tarroni, C. Zannoni, *Mol. Phys.* **61**, 1161 (1987).

[19] A. Polimeno, G. Saielli, P.L. Nordio, *Chem. Phys.*, accepted for publication.

[20] B.J. Berne, in *Physical Chemistry, an Advanced Treatise* ed. by H. Eyring, O. Henderson and W. Jost, Academic Press, N.Y. 1971, vol. VIII B, p. 540.